university of groningen / faculty of science and engineering

A techno-economic feasibility study of phenylalanine production from tertiary cellulose as a building block for alkyds utilizing cellulase and *Corynebacterium glutamicum*

Master's Research Project

Author

Fabian Axmann, S3485722

Supervisors

Prof. dr. G.J.W. Euverink

Prof. dr. J. Krooneman

Abstract

This study explores the enzymatic hydrolysis of tertiary cellulose for glucose production and its subsequent fermentation to phenylalanine using a genetically optimized *Corynebacterium glutamicum* strain for the production of alkyds. Results reveal that a 13% cellulase concentration efficiently achieves a 70% yield of glucose from cellulose, being lower than the anticipated 90% yield in existing literature. Glucose yields from washed and unwashed tertiary cellulose were consistent, indicating no significant impact of the cellulose purification process on the yield. Additionally, the type of buffer (phosphate or acetate) used in enzymatic hydrolysis did not significantly affect the glucose production. A *C. glutamicum* mutant, engineered through UV mutagenesis, showed consistent phenylalanine production across various glucose substrates derived from tertiary cellulose, suggesting that the glucose's source—whether from pure or tertiary cellulose—does not significantly influence the phenylalanine yield. Economic analysis confirmed the feasibility of phenylalanine production from tertiary cellulose-derived glucose on production scales of 1, 5, and 8 kton/year, emphasizing the cost-effectiveness of enzymatic over acid hydrolysis. Although the production cost were found economically feasible for large-scale operations, the economic attractiveness for producing alkyds from phenylalanine remains uncertain, as the target cost needs to be substantially lower.

Contents

Abbreviations

CAPEX	Capital expenditures
CEPCI	Chemical engineering plant cost index
g/c ratio	glucose/cellulose ratio
G-PC	glucose from pure cellulose by enzymatic hydrolysis
G-PC-AC	glucose from pure cellulose by enzymatic hydrolysis on acetate buffer
G-PC-PH	glucose from pure cellulose by enzymatic hydrolysis on phosphate buffer
G-TC	glucose from tertiary cellulose by enzymatic hydrolysis
G-TC-AC	glucose from tertiary cellulose by enzymatic hydrolysis on acetate buffer
G-TC-AH	glucose from tertiary cellulose by acid hydrolysis
G-TC-PH	glucose from tertiary cellulose by enzymatic hydrolysis on phosphate buffer
G-WTC	glucose from washed tertiary cellulose by enzymatic hydrolysis
OPEX	Operating expenditures
PC	Pure cellulose
PG	Pure glucose
TC	Tertiary cellulose
WTC	Washed tertiary cellulose
WWTP	Wastewater treatment plant

1 Introduction

1.1 Alkyds and its potential for a green economy

In the quest for sustainability, the chemical industry is undergoing a transformation. Embracing biobased alternatives and innovative technologies, this shift also aims to align the production of paints and coatings with the principles of a green economy. Paints and coatings consist for ∼44% of resins, of which 20% is based on alkydes. Alkyd resins are a type of polyester resin that is particularly used in the production of coatings and paints. They are synthesised through a reaction between polyols (alcohol with multiple hydroxyl groups), dicarboxylic acids or their anhydrides, and fatty acids or triglycerides. Alkyds offer good penetration into wood, ensuring excellent protection and a naturally high gloss finish. Characteristics of alkyd coatings include their good adhesiveness, hardness, chemical resistance, durability, and ability to cross-link upon exposure to air, facilitated by reaction with oxygen. This eliminates the need for additional cross-linking agents. Crosslinking is a chemical process that forms a network of polymer chains that improves the mechanical properties and chemical resistance of the coating (Hofland, 2012).

Alkyds are synthesised from a blend of components that includes phthalic anhydride (or acid), fatty acids or triglycerides, and polyols such as glycerol or pentaerythritol. These resins have been valued for their effective binding properties that contribute to the protective and aesthetic qualities of finishes. Fatty acids or triglycerides, sourced from natural oils, give alkyds a significant biobased content, aligning them with eco-friendly principles to some extent (Ifijen et al., 2022).

However, the conventional alkyd formulation is not without its reliance on fossil resources, primarily in the form of phthalic anhydride and, in some formulations, benzoic acid. Recognising this, Covestro has developed a technique to reformulate alkyd resins in a more sustainable way. This technique involves the synthesis of novel imide structures from amino acids. These structures are obtained through the reaction of the amino acid with succinic acid and citric acid, yielding monoacid and diacid compounds, respectively. These new compounds are poised to replace the conventional benzoic acid and phthalic anhydride, steering the alkyd composition towards a more sustainable and biobased orientation (Lansbergen et al., 2015).

1.2 Phenylalanine as a building block for alkyds

Amino acids such as glycine, lysine, alanine, and phenylalanine could play a role in the development of sustainable alkyds. Its integration into alkyd production, particularly in the creation of imide structures, signifies a greener approach to coating formulations. This method allows for the substitution of petrochemical components with more sustainable ones, even enhancing the final product's hardness, water resistance, and biobased content. The innovative application of a developed technology for the production of alkyds from imid structures shows its potential to improve the performance of alkyd resins while contributing to environmental sustainability (Lansbergen et al., 2015). For the production of these imid structures, phenylalanine has been the preferred amino acid source because of its high hardness, good water resistance, and high biobased content, due to its high molecular weight. Although the technology has been patented, it has not yet been commercialised due to the high costs of phenylalanine (10-20 €/kg), making it unattractive from an economic point of view. Therefore, the challenge of the developed technology lies in the production of phenylalanine at a lower price to make the process profitable. A significant factor that influences the high price of phenylalanine is the raw materials, accounting for 46% of the operating costs, where glucose is

the most expensive raw material, accounting for 50% of the raw material costs (Pérez-Sánchez et al., 2021),(Brian et al., 1997).

1.3 Tertiary cellulose

Wastewater treatment plants (WWTPs) recognise the value of the cellulose present in the wastewater streams concentrated within, primarily from toilet paper, termed 'tertiary cellulose'. The Netherlands is notable for its exceptionally high cellulose content in wastewater, approximately 250 mg / l (Liu et al., 2022), representing approximately one-third of the total suspended solids (Ahmed et al., 2019). However, traditionally, this cellulose has been underutilized, often ending up incinerated or landfilled. The Cellvation technology, as highlighted by the Dutch Water Sector, introduces a transformative approach to harnessing this resource (Sector, 2024). It involves primary filtering to remove large impurities, followed by advanced methods to isolate cellulose fibres through processes such as flocculation and flotation, ending in a purification stage to ensure the quality of the cellulose for subsequent applications (Lapointe et al., 2022). This system offers a sustainable alternative to primary cellulose sources and aligns with circular economy principles, converting a once-overlooked waste product into a valuable and eco-friendly resource. A possible pathway is the valorisation of tertiary cellulose to glucose to produce phenylalanine by fermentation.

1.4 Production of glucose from cellulose

Production of glucose from tertiary cellulose is the first step in the valorisation of wastse cellulose and is carried out by hydrolysing, increasing the value from almost no value to approximately 0.40 €/kg at the wholesale price (Pérez-Sánchez et al., 2021). Hydrolysis is a chemical reaction involving water that breaks down complex molecules into simpler ones. In the context of cellulose, hydrolysis targets the -1,4-glycosidic bonds connecting glucose units in the cellulose chain, resulting in the release of glucose monomers.

Acid hydrolysis
Acid hydrolysis involves treating cellulose with an acid, typically sulfuric or hydrochloric acid, under controlled conditions of temperature and pressure. The acid acts as a catalyst, breaking down the cellulose chains into glucose units (Qi et al., 2023). The reaction is efficient, but it can be challenging to control, with risks of producing unwanted byproducts or degradation of glucose into hydroxymethylfurfural (HMF) under harsh conditions. The chemistry of the process demonstrates how a nonbiotechnological approach can effectively depolymerise cellulose (Fig. 1). Negative aspects of acid hydrolysis are the need for acid recovery, corrosion in industrial equipment, and the environmental impact of acid disposal (Rinaldi and Schüth, 2009).Yields of 20% are reached for acid hydrolysis, with a reaction time of only 2 hours and a reaction temperature of 140°C (Morales-delaRosa et al., 2014).

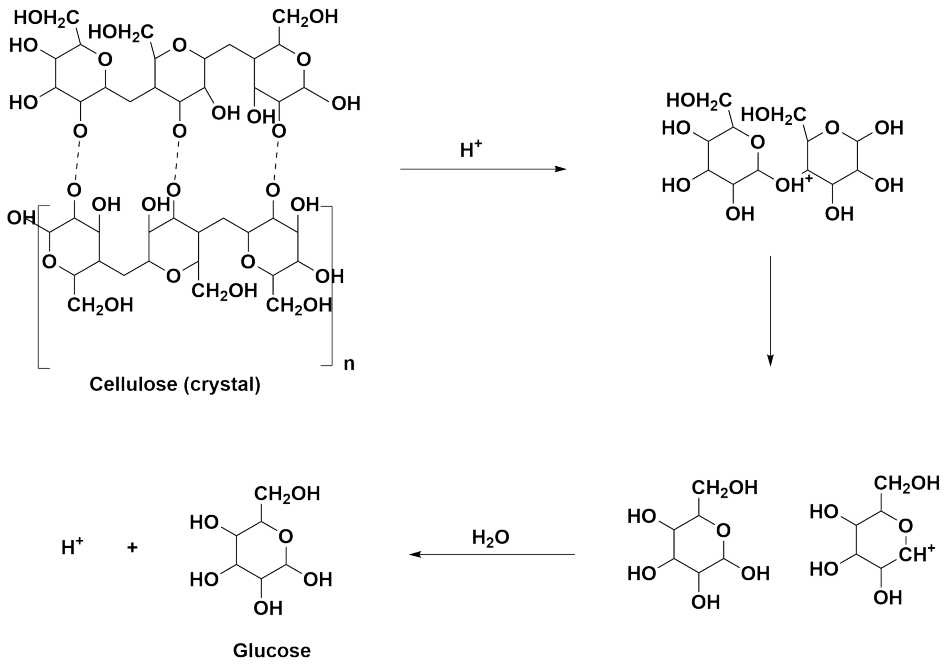

Figure 1: Reaction pathway of gluocose from cellulose by acid hydrolysis

Enzymatic hydrolysis

Enzymatic hydrolysis uses enzymes, typically cellulases, to break down glycosidic bonds in cellulose. The process begins with endocellulases, which cleave the cellulose at random points, primarily targeting its less-ordered regions and yielding longer oligosaccharide chains. Subsequently, they are broken down into shorter chains by exocellulases, which methodically act to release smaller sugars, primarily cellobiose. The final step is facilitated by β-glucosidases, which efficiently convert cellobiose into glucose (Fig. 2) (Anoop Kumar et al., 2018). This method is highly specific, operating under milder conditions than acid hydrolysis, and producing fewer by-products. The enzymes act catalytically to break down the cellulose into glucose. The enzymatic route is innovative due to its specificity, efficiency, and potential for integration into biorefinery frameworks, where even eventual enzyme recycling and reuse can enhance process sustainability (Walker and Wilson, 1991). Yields of 90% are reached for the enzymatic hydrolysis of pure cellulose, with a reaction time of approximately 48 hours and a reaction temperature of 50°C (Yeh et al., 2010), showing a high potential for the hydrolysis of waste cellulose. Despite the higher yield associated with enzymatic hydrolysis, a significant drawback is the cost of cellulase enzymes, which range from \$45 to \$60 per kg, making it unclear and depending on the process whether enzymatic or acid hydrolysis presents a better economic choice for the overall process (Taiwo et al., 2023). In the enzymatic hydrolysis of cellulose, maintaining the optimal pH for cellulase activity, typically around 5.0, yields the highest enzyme activity. Therefore, buffers play an important role in the enzyme activity during the reaction. Two potential buffers are an acetate and a phosphate buffer. The acetate buffer, effective within a pH range of 3.6 to 5.6, aligns well with the optimal pH of the cellulase, potentially improving the hydrolysis efficiency and glucose yield (Cheng, 1998). However, phosphate buffer, despite its broader pH range of 5.8 to 7.4, is frequently used in fermentation media, suggesting practical advantages for subsequent bioprocessing steps. While it may

not perfectly match the cellulase's optimal pH and could result in lower hydrolysis yields, its compatibility with downstream fermentation processes might simplify integrated bioprocess workflows.

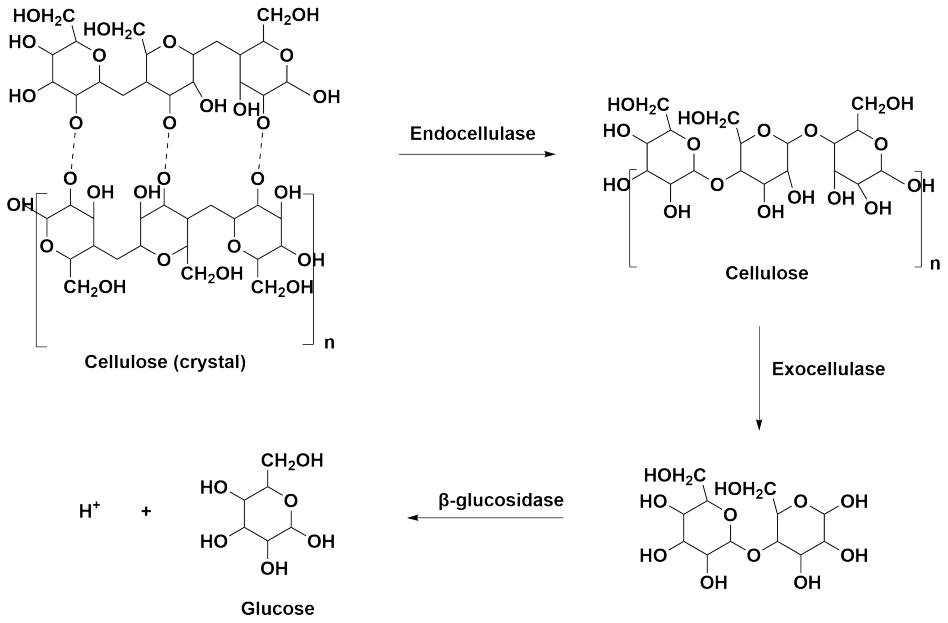

Figure 2: Reaction pathway of gluocose from cellulose by enzymatic hydrolysis with cellulase

Production of glucose from tertiary cellulose

Hydrolysis of waste cellulose for glucose production has already been researched for several years, with cellulose in the form of food, fuel, chemicals or corn stover sometimes being pre-treated with HCl, sulfuric acids or other acids, in order to disrupt the crystalline structure of cellulose, increasing its porosity and surface area, making the cellulose more accessible to enzymes (Mandels et al., 1974),(Spano et al., 1976). Recently, interest has increased for the hydrolysis of cellulose captured from wastewater, and technologies are being developed for the efficient filtration and capture of cellulose in wastewater treatment plants (Libardi et al., 2022). The hydrolysis of waste cellulose has also been used for fermentation purposes already, mainly for the production of bioethanol (Brethauer and Wyman, 2010), (Achinas et al., 2019). The use of enzymes versus sulfuric acid plays an important role in environmental evaluation. Despite the high cost of enzymes—even when produced in-house—the sustainability angle favours enzymatic hydrolysis. If a method is developed to efficiently separate acetic acid (e.g., using catalytic or anion exchange resins), the remaining waste could be safely discharged into sewage systems, offering an environmentally friendly advantage (Sun et al., 2013). In contrast, acid hydrolysis with sulfuric acid generates numerous by-products that require costly disposal methods, which have a negative impact on the environmental sustainability of the process.

1.5 Production of phenylalanine from glucose

The production of glucose-derived phenylalanine increases the economic value when comparing the costs of glucose (0.4 €/kg) and phenylalanine (10-20 €/kg).

The shikimate pathway and phenylalanine synthesis

Phenylalanine is produced by *Corynebacterium glutamicum* via the shikimate pathway, a

metabolic pathway within microorganisms that facilitates the production of aromatic amino acids, including phenylalanine. This pathway transforms phosphoenolpyruvate (PEP) and erythrose-4-phosphate (E4P), derivatives of glucose metabolism, into various aromatic compounds, phenylalanine being one of the end products (Haslam, 1993).

The process begins with the enzyme 3-deoxy-D-arabinoheptulosonate 7-phosphate synthase, catalysing the initial step that combines erythrose-4-phosphate and phosphoenolpyruvate. Following this, a sequence of enzymatic transformations follows, involving the enzymes 3-dehydroquinate synthase, 3-dehydroquinate dehydratase, and $NADP^+$-dependent shikimate dehydrogenase, leading to the formation of shikimate. Subsequent enzymatic actions facilitated by shikimate kinase, 5-enolpyruvyl-shikimate-3-phosphate synthase, and chorismate synthase steer the pathway towards producing chorismate, the precursor for phenylalanine synthesis. Other enzymes in the shikimate pathway are NAD^+ and 3-dehydroshikimate dehydratase, which play a role in the pathway, but do not lead to the production of phenylalanine (Haslam, 1993). After the production of chorismate, the biosynthesis of L-phenylalanine (L-Phe) involves three enzymatic steps. Initially, chorismate undergoes a transformation catalysed by chorismate mutase, which converts it into prephenate. This step marks the divergence from chorismate to specific pathways that lead to different aromatic amino acids. The enzyme prephenate dehydratase (PDT) then acts on prephenate, catalysing its conversion to phenylpyruvate through a decarboxylation and dehydration process. This reaction is steering the pathway specifically towards L-Phe synthesis. Subsequently, the enzyme aromatic amino acid aminotransferase facilitates the transfer of an amino group from L-glutamate to phenylpyruvate, forming L-Phe. A different route is the production of phenylalanine from chorismate facilitated by the enzymes phrephenate aminotransferase and arogenate dehydratase (Fig. 3).

Feedback activation and inhibition

In the shikimate pathway, several enzymes play an important role through feedback mechanisms. These enzymes catalyse or inhibit specific reactions leading to the formation of intermediates and end products. These feedback mechanisms can be split into feedback activation and feedback inhibition. This regulation prevents the overaccumulation of aromatic amino acids, which could lead to toxic effects, disrupting cellular balance, and potentially causing cell death. By fine-tuning enzyme activity, these feedback controls ensure the efficient use of metabolic resources, maintaining cellular health and viability.

Activation:

Chorismate mutase (CM) and Arogenate dehydratase (ADT) are subject to regulatory activation by aromatic amino acids: tryptophan activates CM, increasing the flux toward phenylalanine and tyrosine synthesis, whereas tyrosine is known to activate ADT, redirecting the flux of the pathway towards phenylalanine production (Yokoyama et al., 2021).

Inhibition:

The enzyme DAHP synthase is inhibited by the end products phenylalanine, tyrosine, and tryptophan (Herrmann, 1995). Anthranilate synthase (AS), which leads the pathway toward tryptophan synthesis, is inhibited by tryptophan itself. Furthermore, chorismate mutase is inhibited in the presence of its product's downstream metabolites, phenylalanine and tyrosine (Lütke-Eversloh and Stephanopoulos, 2005). Similarly, phenylalanine has an inhibitory effect on ADT, regulating its own synthesis through a feedback loop. Additionally, TyrA, an enzyme that contributes to tyrosine synthesis, is feedback inhibited by tyrosine (Yokoyama et al., 2021).

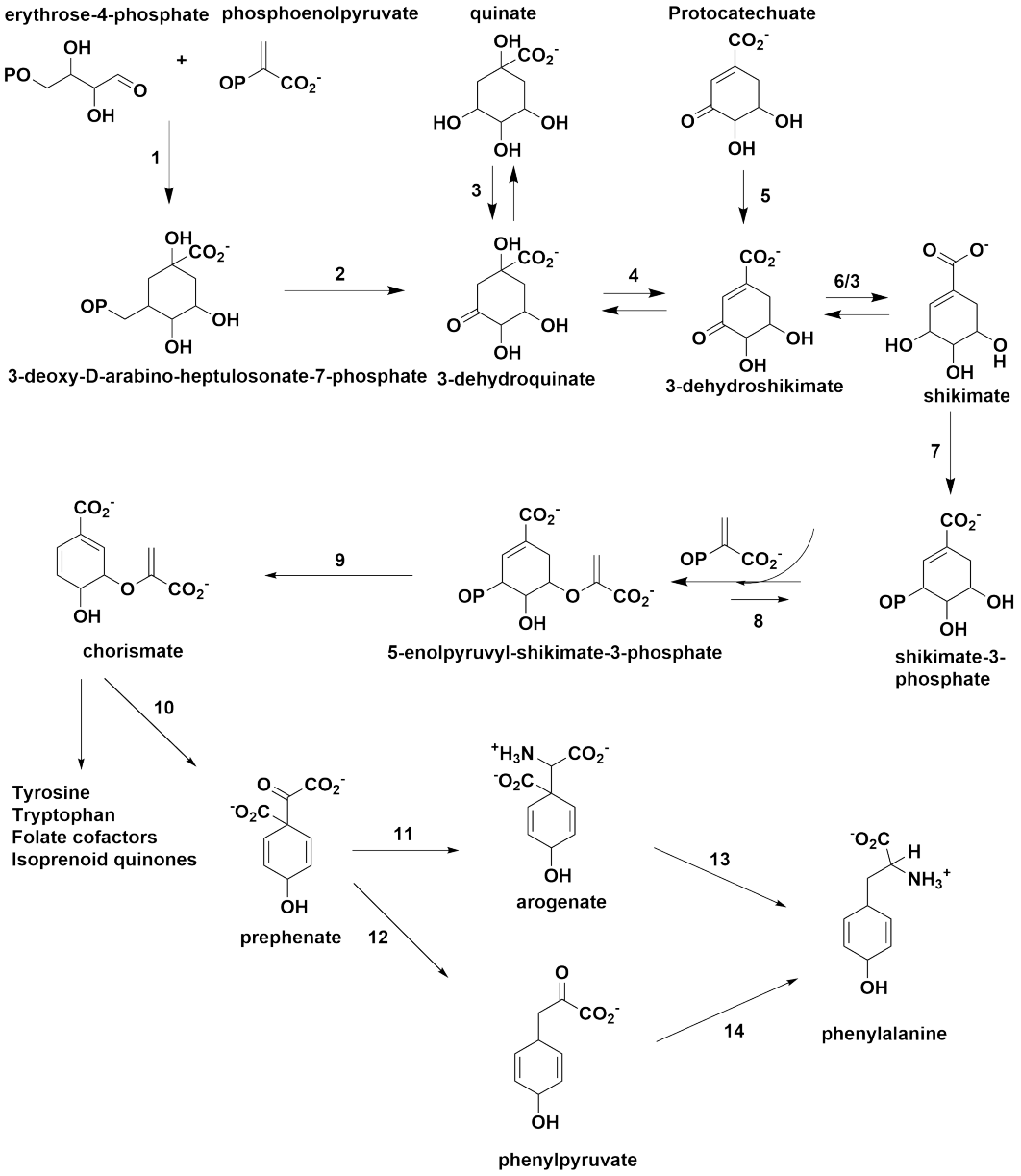

Figure 3: Reaction pathway of phenylalanine from E4P and PEP following the shikimate pathway. 1, 3-deoxy-D-arabino-heptolusonate 7-phosphate synthase; 2, 3-dehydroquinate synthase; 3, NAD^+ or PQQ-dependent quinate/shikimate dehydrogenase; 4, 3-dehydroquinate dehydratase; 5, 3-dehydroshikimate dehydratase; 6, $NADP^+$-dependent shikimate dehydrogenase; 7, shikimate kinase; 8, 5-enolpyruvyl-shikimate-3-phosphate synthase; 9, chorismate synthase; 10, chorismate mutase; 11, prephenate/aromatic amino acid aminotrasferase; 12, prephenate/-cyclohexadienyl dehydratase; 13, arogenate/cyclohexadienyl dehydratase; 14, prephenate/aromatic amino acid aminotransferase

Strain engineering

The engineering of strains of *C. glutamicum*, to optimise this pathway, shows progress in metabolic engineering and bioprocess technology. These strains are genetically mutated to en-

hance the flux through this pathway, efficiently directing it towards phenylalanine production and reaching phenylalanine production up to 20 g/l (Shu and Liao, 2002). This optimisation is important for the industrial-scale synthesis of phenylalanine, where its efficiency, yield, and cost-effectiveness are assessed. To enhance phenylalanine production through strain improvement of *C. glutamicum*, various strategies have been used, focussing on genetic modifications and process optimisation to increase yield and efficiency. For example, the integration of the bifunctional enzyme chorismate mutase-prephenate dehydratase from *E. coli* into *C. glutamicum* and subsequent optimisation of the oxygen supply in the fermentation process have been used to enhance phenylalanine production. The introduction of the pheA gene into *C. glutamicum* significantly increased the relevant enzyme activities, leading to an 35% increase in phenylalanine levels, with concentrations achieving up to 23 g/L. Furthermore, adjusting oxygen transfer rates in fermentation of a high-producing *C. glutamicum* strain demonstrated that optimised oxygen availability could mitigate feedback inhibition, achieving concentrations as high as 23.2 g/L (Ikeda et al., 1993),(Shu and Liao, 2002).

Random strain mutation and selection using F-phenylalanine
An easier method for mutating a *C. glutamicum* strain for enhanced phenylalanine production involves random mutagenesis, executed by UV-C exposure. The selection of phenylalanine-overproducing strains is facilitated using the amino acid analogue F-phenylalanine. This analogue can be used in isolating mutants with deregulated prephenate dehydratase (PDT) enzymes, crucial in the phenylalanine biosynthesis pathway.

Mutants resistant to F-phenylalanine are indicative of alterations in PDT enzyme regulation or activity, manifesting in several distinct forms: resistance to L-phenylalanine feedback inhibition, deregulated or constitutive enzyme synthesis, altered enzyme kinetics with decreased Km for prephenate, or a combination of these (Fazel and Jensen, 1979). Such modifications enable strains to avoid normal feedback inhibition mechanisms, potentially leading to elevated phenylalanine production. Resistance to feedback inhibition implies that these mutants can maintain high levels of enzyme activity despite the presence of end-product phenylalanine, which would typically suppress the pathway. This is evidenced by mutants exhibiting a complete or partial loss of sensitivity to L-phenylalanine's inhibitory effects, maintaining significant enzyme activity or displaying altered regulatory properties that are helpful for phenylalanine synthesis (Euverink, 1995).

Research on mutant strains resistant to phenylalanine analogues, such as p-fluorophenylalanine (PFP), showed the potential for strain selection. A *C. glutamicum* strain, after mutagenic treatment, showed the ability to produce phenylalanine, yielding up to 9.5 g/L (Hagino and Nakayama, 1974). Also, in (De Boer and Dijkhuizen, 2005), a *C. glutamicum* strain was isolated using p-fluorophenylalanine resulting in a phenylalanine production of 12.5 g/l, indicating a promising route for strain selection.

The potential of auxotrophic mutants
Besides strain optimisation, there are other strategies to reduce the cost of phenylalanine production. An approach explored the in vitro reconstruction of the phenylalanine biosynthesis pathway in *E. coli*, by using the shikimate's pathway enzymes without the use of microorganisms. By analysing the impact of excess of different enzymes, the study by Ding et al. quantitatively analysed the impact of enzyme concentrations on phenylalanine yields, revealing that increasing specific enzymes could significantly boost production. By enhancing the levels of shikimate kinase (AroL) and EPSP synthase (AroA) 2.5 times, the phenylalanine

yield increased, with in vivo experiments showing a production reaching 62.47 g/L (Ding et al., 2016). While replicating this enzyme-driven process on an industrial scale might be expensive due to the high amount of enzymes required, an alternative could be creating an auxotrophic mutant that produces enzymes up to a certain absorbance. Beyond this point, the carbon source will be redirected from biomass growth to increased product yield, offering a strategic method to improve production efficiency.

Production of phenylalanine from tertiary cellulose
Another possibility of reducing the cost of phenylalanine production involves the use of cheaper substrates; converting tertiary cellulose into glucose presents a cost-effective source of raw materials. This approach aligns with the broader goal of making phenylalanine production more economically viable for applications within the alkyd resin production by Covestro. The company's interest lies in assessing the technical feasibility and cost per kilogramme of phenylalanine at production scales of 1 and 5 kilotons annually. Given the relatively small scale of this operation compared to other fermentation processes, this research also considers the implications of scaling up to 8 kilotons per year. The goal is to evaluate whether the production of phenylalanine from tertiary cellulose can meet the cost targets necessary to render the novel alkyd production technique economically feasible, thereby supporting the transition toward more sustainable industrial practices.

1.6 Research questions

In this research, an alternative biotechnological route for the production of phenylalanine is sought. It starts from readily available and cheap renewable resource waste cellulose. The waste cellulose is converted to glucose by enzymatic hydrolysis, and the resulting glucose is converted to phenylalanine using a *C. glutamicum* strain. The research questions are listed below, where the metabolic and growth parameters considered are phenylalanine production, glucose consumption, OD_{600}, and ammonia concentration.

R1: What differences in metabolic and growth parameters are observed when cultivating a phenylalanine-producing strain of *Corynebacterium glutamicum* on glucose derived from enzymatic hydrolysis of tertiary cellulose using cellulase compared to pure glucose?
R1.1: If there are, what are the differences in glucose yield by enzymatic hydrolysis of tertiary cellulose, washed tertiary cellulose, and pure cellulose using cellulase?
R1.2: If there are, what differences in glucose production and process design are observed when using cellulase for enzymatic hydrolysis of tertiary cellulose in an acetate buffer versus a phosphate buffer?
R1.3: What are the observed differences in metabolic and growth parameters during fermentation of a phenylalanine-producing strain of *C. glutamicum* with glucose from G-(W)TC-AC, G-(W)TC-PH, and G-TC-AH compared to glucose from pure cellulose and pure glucose?

R2: Considering a production capacity of 1, 5, and 8 kilotons of phenylalanine per year, what are the estimated costs per kilogramme of phenylalanine production from tertiary cellulose sourced from wastewater treatment plants?
R 2.1: What does the industrial-scale process design entail, and what are the estimated costs per kg glucose when producing glucose from tertiary cellulose through enzymatic and acid hydrolysis when considering a phenylalanine production capacity of 1, 5, and 8 kton/year?
R 2.2: What does the industrial process design entail and what are the estimated costs per kg of phenylalanine when producing phenylalanine by fermentation with a phenylalanine-producing strain of *C. glutamicum* when considering a phenylalanine production capacity of

1, 5, and 8 kton/year?

1.7 Hypotheses

Hypotheses for the research questions are provided below:

H1: It has been proven by literature that the enzymatic conversion of cellulose to glucose and the subsequent fermentation to phenylalanine will be technically feasible. Therefore, no significant differences are expected in the fermentation process efficiency or phenylalanine yields when using glucose derived from tertiary cellulose compared to pure cellulose. This expectation is based on the assumption that glucose, regardless of its source, should serve as an equivalent substrate for the phenylalanine-producing strain of *C. glutamicum*.

H1.1: It is expected that washing tertiary cellulose will effectively remove soluble impurities but will convert cellulose to glucose with the same yield, regardless of the purity of the cellulose substrate.

H1.2: It is expected that the enzymatic hydrolysis of tertiary cellulose will yield higher glucose concentrations in an acetate buffer than in a phosphate buffer, due to the optimal pH condition (pH 5.0) for cellulase activity to be more stably maintained by the acetate buffer.

H1.3: The removal of soluble impurities is expected to enhance phenylalanine production, assuming that such impurities could interfere with the metabolic pathways or growth of *C. glutamicum*. If not removed in the process, the buffer and other chemicals used during G-TC-AC, G-TC-PH, and G-TC-AH are expected to influence metabolic pathways and growth, where the glucose produced in the presence of a phosphate buffer is assumed to obtain the highest phenylalanine yield, and as the same buffer is present in the medium, these changes in metabolism are expected to be less than the acetate present from the acetate buffer or other chemicals present after acid hydrolysis.

H2: The scales on which the process will be designed (1, 5, and 8 kilotons per year) are expected to be relatively small compared to the industry, making it harder to compete with the market. Nevertheless, it is expected that producing phenylalanine from glucose derived from tertiary cellulose on an industrial scale will be cost-effective, significantly reducing the cost per kilogram of phenylalanine in comparison with phenylalanine costs on the market.

H2.1: The industrial-scale process design for the production of glucose from tertiary cellulose is expected to be economically advantageous compared to the price of glucose on the market. Here, glucose production by acid hydrolysis is expected to be more cost-efficient than enzymatic hydrolysis due to its significantly faster reaction time (2 vs. 48 hours) and the anticipated high costs associated with the acquisition of cellulase.

H2.2: The industrial-scale production of phenylalanine from the phenylalanine-producing strain of *C. glutamicum* using glucose from tertiary cellulose is expected to result in a reduced cost per kg of phenylalanine in comparison with the price on the market. This cost reduction is expected due to the low-cost substrate (tertiary cellulose) and the elimination of the profit margin required when purchasing phenylalanine from external suppliers. The production on the higher scales is expected to further increase the cost-effectiveness through economies of scale.

2 Materials & methods

2.1 Analytical methods

Glucose assay

To determine the glucose concentration during glucose and phenylalanine production, the Megazyme D-Glucose Assay Kit (GOPOD format) was used in a 96-well microtiterplate. This assay contains glucose oxidase, peroxidase, p-hydroxybenzoic acid, and 4-aminoantipyrine. Here, glucose reacts with oxygen, water, and glucose oxidase to D-gluconate and hydrogen peroxide. Subsequently, the hydrogen peroxide produced reacts with p-hydroxybenzoic acid, 4-aminoantipyrine, and peroxidase to Quinoneimine; a dye that can be quantified using photospectrometry at λ=510 nm. The assay was used within its linear range, which is between 0.0-1.0 g/l glucose when adding 10 µl sample to 300 µl reagent. The absorbance was measured after adding and mixing the reagent with the sample and sealing and incubating the microtiter plate at 40°C for 30 minutes. The calibration line was made with samples in triplicate. The experimental samples were analysed in duplicate.

Individual volatile fatty acids assay

The presence of acetic acid in the glucose solution produced was determined using a TLC assay (Robert-Peillard et al., 2019), which was developed for the low-cost and easy determination of individual volatile fatty acids. The mobile phase was made of a mixture of cyclohexane and ethyl acetate (40/60, v/v). Thin-layer chromatography plates (aluminum/silica, 20 x 20 cm) were used. First, 300 µl HOAT + EDAN solution was mixed with 40 µl EDC and 250 µl sample in a 1.5 ml Eppendorf cup. After 5 minutes of waiting, 75 µl K_2PO_4 was added and mixed. After waiting 1 minute, 3 µl of the prepared solution was spotted on the TLC sheet, 1 cm above the bottom and 1 cm from each other. Following the drying of the plate with a hair dryer set to medium heat, the TLC sheet was immersed in the mobile phase. After 30 minutes, the front developed to a maximum of 1 cm below the top of the plate and the sheet was removed and dried. After the sheet was dried using a hair dryer at medium heat, the TLC plate was sprayed with a PMA solution, after which the eventual presence of acetic acid (and other individual volatile fatty acids) in the sample became visible directly. A sample of the acetic acid buffer used in glucose production was used as a standard. Acetic acid was activated using the reaction shown in Fig. 4. The EDC and HOAT solution ensure activation of the fatty acid at low pH. The EDAN solution amidiates the activated acid. $Rf - NH_2$ is a fluorescent amine that was stained using the PMA solution. For this assay, the HOAT + EDAN solution consisted of 6 g/l 7-aza-1-hydroxybenzatriazole (HOAT) and 2 g/l N-(1-naphthyl)ethylenediamine (EDAN) in Milli-Q water with a final pH set at 3.6. The EDC solution consisted of 100 g/l N'(3-dimethylaminopropyl)-N-ethylcarbodiimide) in absolute ethanol. The KH_2PO_4 solution serving as pH buffer consisted of 0.25 M KH_2PO_4 in 0.35 M NaOH solution. The PMA solution consisted of 3% w/v phosphomolybdic acid hydrate in water.

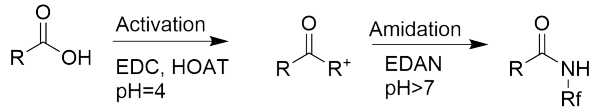

Figure 4: Reaction scheme of reaction during the activation and amididation step during the VFA assay described by Robert-Peillard et al. (2019)

Amino acid assay
To identify and quantify the presence of phenylalanine and other amino acids, the TLC assay described in Pachuski et al. (2002) was used. For this assay, 1% (w/v) ninhydrin in pure ethanol was used as the staining solution. The mobile phase consisted of a mixture of n-butanol:acetic acid:water (3:1:1, by volume). Three microlitres of the sample were spotted on the TLC plate, which was subsequently dried using a hair dryer set to medium heat. Subsequently, the TLC plate was immersed in the mobile phase for approximately 45 minutes. The plate was then dried using a hair dryer at medium heat, and stained with ninhydrin using a spray bottle until the plate was completely covered. Subsequently, the plate was placed on a tissue layer in a drying oven at 60°C for 30 minutes. The amino acid was identified and quantified using the online software 'Justquantify' which measures the intensity of a spot. To quantify, a calibration curve was made on the same silica sheet as the samples. Here, it should be kept in mind that the quantification is highly dependent on the accuracy of the pipets used and therefore could vary.

Ammonia assay The ammonia concentration during fermentation was determined using an assay provided by Megazyme that contains measurements using photospectrometry in a 96-well microtiterplate. The assay was used within the linear range between 0-70 mg/l ammonia. An aliquot of NADPH solution (30 µl), 2-oxoglutarate (20 µl), and water (180 µl) was added to each well. After mixing and waiting 2 minutes, the absorbance was measured at λ=340 nm, to quantify the presence of NADPH. Subsequently, 2 µ l glutamate dehydrogenase solution and 20 µl water were added to each well, facilitating the reaction between NADPH and 2-oxoglutarate to produce L-glutamic acid, $NADP^+$, and water. After 5 minutes of waiting, the absorbance was measured, after which every minute the plate was stirred and measured until the absorption values increased again, implying that all ammonia had reacted and thus could be measured by measuring absorbance again at λ=340 nm. The consumption of NADPH is stoichiometric for the amount of ammonia present. The ammonia amount was quantified by subtracting the absorbance of the second measurement from the first measurement.

2.2 Production of glucose utilising cellulase
Cellulose was hydrolysed enzymatically using Cellic Ctec2, a cellulase enzyme supplied by Sigma-Aldrich. The enzyme demonstrates optimal activity at 50°C and a pH of 5.0 (Novozymes, 2010). To evaluate the efficiency of glucose production, three cellulose variants were used as substrates: pure cellulose, tertiary cellulose, and washed tertiary cellulose. Pure cellulose acted as a control to determine whether variations in subsequent production stages were attributable to the glucose production process itself or the constituents within the tertiary cellulose. The use of washed tertiary cellulose was intended to assess the impact of potential contaminants on the conversion efficiency to glucose and phenylalanine. Two pH buffers were tried; an acetate and phosphate buffer. The selection of the acetate buffer was guided by its ability to inhibit bacterial consumption of the generated glucose, and thus the procedure did not have to be performed under sterile circumstances. The phosphate buffer was found to be promising as, although sterile circumstances are assumed to be necessary, the risk of inhibiting subsequent fermentation processes was minimised with the phosphate buffer, in contrast to the acetate buffer, which might inhibit microbial growth.

2.2.1 pH buffers
Acetate buffer
The acetate buffer was found to be effective within a pH range of 3.6-5.6. This pH range aligns with the optimal conditions for the cellulase enzyme used in the process (Swamy and Jaffe,

1983). The buffer solution was composed of 0.2 M acetic acid and 0.35 M sodium acetate, diluted in water, and its pH was adjusted to 5.0 using NaOH. Both acetic acid and sodium acetate were added to ensure sufficient amounts of both tha acid and its conjugate base, enhancing the buffer's capacity to maintain the pH at 5.0. The high concentration of acetic acid was chosen to prevent the consumption of the glucose produced by microorganisms.

Phosphate buffer
The phosphate buffer used during the enzymatic conversion of cellulose to glucose is the same as the buffer used in the media in the phenylalanine production step. It is suitable within the pH range of 5.8-7.4 (Gomez et al., 2001). The phosphate buffer consisted of 100 g/l KH_2PO_4, and 200 g/l K_2HPO_4 and was brought to pH 5.8 using NaOH.

2.2.2 Washing tertiary cellulose

Prior to washing, the mass of tertiary cellulose was determined. Subsequently, 3 grammes of this material was introduced into a large beaker containing 2 litres of Milli-Q water and stirred for one hour. Given the insolubility of cellulose, it was necessary to immerse the material repeatedly beneath the water surface to ensure thorough saturation and submersion. This process was facilitated by vigorous immersion during the stirring phase. Subsequently, the material was filtered using the Büchner apparatus, as shown in Fig. 25. After filtration, the material was placed in an ultrasonic bath with 1 litre of water maintained at 25°C for an additional hour, after which Büchner filtration was used once more.

2.2.3 Defining weight of water content and soluble impurities in cellulose and glucose

As yield was defined by the grammes of glucose produced over the grams of cellulose at t=0, the water content in 'dry' PC and TC was determined to account for this when calculating the yield. To quantify the effect of washing on the soluble impurities present, the weight of soluble impurities lost after washing was defined. To quantify the weight of soluble impurities in TC that were removed by washing, 3 grammes of TC were weighed and subsequently dried. The weight decrease was observed as m1, representing the water content in 3 grammes of dry mass. Subsequently, another 3 grammes of TC was weighed (m2), washed, dried again, and reweighed to obtain m3. The weight difference minus the water content in the dry material (m2-m3-m1) signifies the weight of soluble impurities removed.

The amount of soluble impurities present in the produced glucose was found by defining the theoretical glucose weight by its concentration and subtracting this from its dry weight after vacuum distillation. It was assumed that the observed weight difference (m4) of G-PC consist of water and eventually precipitated acetate. Knowing the weights of water and acetate per gramme of glucose, the additional weight difference for G-TC and G-WTC were assumed to be soluble impurities.

The effect of washing on impurity content can be used for defining the feasibility of performing pretreatment washing steps on an industrial scale.

2.2.4 Defining the amount of cellulase needed, and quantifying cellulose content in TC

To be able to compare the glucose production profiles of cellulose, the PC, TC, and WTC samples should contain the same amount of cellulose at t=0. Therefore, it was assumed that PC consisted of 100% cellulose, and it was investigated how much cellulose was present in TC. The necessary enzyme concentration was also defined. This information was found by

producing glucose with 1.5, 3, 13, and 30% (w/w, g enzyme/g cellulose) with 100 mg of cellulose material (PC, TC, and WTC) with 6.5 ml buffer in duplo under optimal conditions (50°C, pH 5.0) Novozymes. 10 ml of buffer was chosen to ensure that the TC was suspended in the tubes to ensure mixing. It was assumed that 30% (w/w) would be excess, to define the maximum yield. Before adding cellulose to the buffer and enzyme mix, a sample t=0 was taken, as the cellulase contains an unknown amount of glucose. An alternative would be to use a g25 column to separate glucose from the enzyme. The samples were incubated in 15 ml tubes with parafilm on the screw to prevent liquid from escaping on a tube rotator at 15 rpm. Each day, samples were taken at the same time for four days. Before analysis, the cellulose in the samples was removed by spinning at 14,000 rpm, as the particles would affect photospectrometric results.

2.2.5 Production of glucose from cellulose

In an acetate buffer

Glucose was produced from PC, TC, and WTC using the enzyme concentration defined in the previous section (13%, w/w), and a normalised amount of PC, TC, and WTC for the defined cellulose concentration in the previous section (1.8, 3, and 3 grammes respectively) to account for variations in cellulose content. Glucose production was performed in triplicate in 50 ml tubes with 45 ml buffer. Insurance for the full suspension of the cellulose was taken into account when determining the cellulose weight. Consideration was given to ensuring cellulose suspension and, thus,effective mixing in the tube rotator when determining the quantity of cellulose. Taking into account the existing water content in WTC, its amount of water was determined by the weight difference between post-washing and pre-washing and the subtraction of the defined impurity content. On the basis of the water content present, a tailored buffer was prepared to match the concentrations and water levels consistent with the buffer used for PC and TC. The glucose solution produced was centrifuged at 20,000 rpm and filter sterilised for fermentation in later experiments. The samples were filter sterilised, as in the autoclave the Maillard reaction was initiated due to the presence of amino acids and glucose in the solution (Fig. 30 in Ap. A).

In a phosphate buffer

A single experiment was carried out in phosphate buffer for 1.8 g PC and 3 g TC. The cellulose and phosphate buffer were autoclaved separately. The enzyme (13%, w / w) was sterilised with a filter. The two 50 ml sterile tubes containing cellulose, buffer, and enzyme were incubated at 50°C and rotated at 15 rpm. The samples were taken each day at the same time for three days in a sterile environment.

Removal of acetic acid from the glucose mixture

Vacuum distillation was performed to remove acetic acid from the glucose solution at 25 mbar and 50°C. As a pretreatment, the mixture was acidified below its pKa value (4.7) using HCl to ensure it was in its uncharged molecular form, as it would not evaporate in its ionised form. After all the liquid had evaporated, the mixture was diluted again, acidified, and evaporated under the same conditions for three cycles to remove as much acetic acid as possible. The individual volatile fatty acid assay was used to confirm the removal of acetic acid. After this trajectory, the remaining dry material inside the round-bottom flask was weighed, after which the glucose was dissolved and the glucose concentration was determined. The glucose concentration and the dry weight were used to determine the weight of the impurities present.

2.3 Production of L-phenylalanine utilizing *C. glutamicum*

2.3.1 Strain

The strain used was *Corynebacterium glutamicum* wild-type DSM 20300. It is known that this strain does not produce phenylalanine.

2.3.2 Cultivation Media

The cultivation medium chosen was a slightly modified version of the mineral medium (MM) described in Bäumchen et al. (2007) (Tab. 1). The medium contains glucose as a carbon source, a fosfate buffer to maintain the pH at 7.2, ammonium chloride as an ammonium source, and protocatechuic acid (PCA) as an iron chelator. Ammonium chloride was used as the ammonium source instead of ammonium sulphate because ammonium chloride was not available in the lab. The concentration was recalculated to have the same amount of ammonia. The concentration of ferrous sulphate was reduced compared to the original amount, as foggy precipitation was formed on the bottom of the flask after one day when 0.01 g/l was used. This might be due to iron oxidation.

Table 1: Components in MM defined by (Bäumchen et al., 2007) with alterations made for this research C. glutamicum

	Bäumchen et al. (2007) (g/l)	MM used (g/l)
D-glucose	10	10
$(NH_4)_2SO_4$	10	
NH_4Cl		8.075
KH_2PO_4	1	1
K_2HPO_4	2	2
$MgSO_4 \cdot 7H_2O$	0.25	0.25
$CaCl_2$	0.01	0.01
$FeSO_4 \cdot 7H_2O$	0.01	0.0005
$MnSO_4 \cdot H_2O$	0.01	0.01
$ZnSO_4 \cdot 7H_2O$	0.001	0.001
$CuSO_4$	0.0002	0.0002
$NiCl_2 \cdot 6H_2O$	0.0002	0.0002
Biotin	0.0002	0.0002
Protocatechuic acid	0.03	0.03

To validate the efficacy of the medium, *C. glutamicum* was grown in mineral medium (MM) and BHI (brain heart infusion, rich medium) in 100 ml Erlenmeyers containing 20 ml of medium in a shaking incubator at 30°C for comparison. The inoculum originated from precultures grown in the same medium in which they were inoculated. Growth was measured by spectrophotometry at $\lambda = 600$ nm (Lira-Parada et al., 2021) after dilution to an OD at a measurement between 0.05-0.4. After growth, the culture broth was inspected under the microscope (*1000) to assess its purity. The reason for the use of a mineral medium instead of BHI is that phenylalanine is present in BHI and thus the amino acid analogue is expected to function less optimally. In addition, it would be more difficult to quantify the production of phenylalanine if it is already present.

2.3.3 Strain optimisation

Random mutation of strain DSM20300 of wild-type *C. glutamicum* was carried out by exposing the bacteria in a small amount of media in a Petri dish to UV-C light in the flow cabinet.

The strain selection was performed using the amino acid analogue F-phenylalanine.

Finding the MIC
To define the amount of F-phenylalanine to add, the MIC should be found. The minimal inhibitory concentration (MIC) is the concentration from which the growth is inhibited. With a too-high concentration of F-phenylalanine, more mutations are expected to be needed to survive. The MIC was found by growing the wild type in Erlenmeyers with different concentrations of F-phenylalanine: 25, 50, 100, 500, 1000, and 2000 µ g /ml.

UV mutagenesis on agar plates
After finding the right amount of analogue and seconds of UV-C exposure, the bacteria were mutated and grown on plates. The plates contained mineral medium and different concentrations of F-phenylalanine: 0, 25, and 50 $\mu g/ml$. 100 µl of inoculum was transferred to the plates at dilutions of x1000 and x100, and exposed to UV-C light for 0, 15, 30, 45, and 60 seconds. The plates were incubated in an incubator at 30°C for a maximum of one week.

Liquid UV-mutagenesis
Liquid mutagenesis was performed by exposure of liquid biomass to UV-C light and growth in liquid media, after which phenylalanine-producing strains were isolated on agar plates containing F-phenylalanine.

Finding the right exposure time
Using the determined MIC, the optimal duration of UV-C light exposure was determined to find the right balance between sufficient irradiation to cause beneficial mutations and avoiding excessive exposure that could result in significant damage or lethality. Mutation should be done with as little exposure time as possible to minimise the number of silent mutations. Also, at a too long exposure time, the bacteria were expected to die. 100µl of biomass in medium that was at the end of its exponential phase was diluted with media to an OD of 2 and added to a Petri dish in the flow cabinet. The UV-C light was turned on below the flow cabinet so that the light could not reach the biomass. After the light was on for 10 seconds, it was placed directly above the Petri dish (10 cm) for a period of 15, 30, or 60 seconds. After mutagenesis, 50µl of the medium was added to an Erlenmeyer containing mineral medium and analogue. Growth was monitored and after one day at max OD, a sample was taken and analysed using the amino acid assay with a standard containing phenylalanine. If a strain was found that produced phenylalanine, 100 µl of diluted (x10 & x100) sample was smeared on an agar plate containing mineral medium and different concentrations of F-phenylalanine, depending on the analogue concentration in the previous medium. Theoretically, bacteria potentially mutated to grow on F-phenylalanine would exhibit enhanced growth rates and, consequently, a greater likelihood for phenylalanine production. Therefore, the largest colonies were selected for isolation.

The colonies picked were grown in 10 ml tubes with 3 ml of media to ensure that there was enough oxygen for the bacteria to grow and produce. After three days, samples were taken and phenylalanine production was evaluated using the amino acid assay on TLC and OD_{600} was measured. Strains were evaluated based on their production of phenylalanine and OD_{600}. The objective was to identify the strain with the highest phenylalanine production; however, strains demonstrating substantial production coupled with a significantly lower OD_{600} were also considered advantageous, indicating that a smaller biomass could produce more phenylalanine.

Second UV-mutagenesis

If a phenylalanine-producing strain was found and isolated, the two most promising strains were mutated again to increase phenylalanine production even more. The mutated bacteria were inoculated in 10 ml tubes with 3 ml of medium. As in the previous mutagenesis, the bacteria adapted to grow in the presence of small amounts of analogue, a higher concentration of analog was used (50, 100, & 200 µg/ml). Based on the previous exposure time analysis, the bacteria were exposed to UV-C for 0, 5, 10, 15, or 20 seconds. Of the two isolated strains in the previous section, 150 µl was exposed to UV-C light for 5, 10, 15, and 20 seconds, after which 50µl was inoculated in 3 ml of medium containing 50, 100, and 200 µg/ml F-phenylalanine. The strains that grew were isolated on agar plates containing medium and different amounts of analogue. Again, the analogue concentration in the plate was dependent on the analog concentration in the media. The analogue concentration in the plate had to be at least the same as the concentration in the medium to preserve selection. After incubation of plates for three days in an incubator at 30°C, the largest colonies were picked from each plate and isolated in 44 10 ml tubes containing 3 ml of liquid medium. After three days of growth, from these colonies, a final colony (H1) was chosen based on its phenylalanine production on TLC, OD_{600}, and UV-C exposure time.

Glycerol stocks Glycerol stocks were made from strains producing phenylalanine by taking 1000 µ l of liquid medium culture at maximum OD (approximately 3-4) in a 2 ml Eppendorf cup, spinning at 5000 rpm, removing the supernatant and adding 500 µ l of a 30% glycerol stock. This was carefully resuspended and placed in liquid nitrogen to prevent cell sedimentation. After two minutes in liquid nitrogen, the Eppendorf cups were put into a -80°C freezer.

Engineering of a tryptophan-dependent phenylalanine-producing strain
This study aimed to develop a bacterial strain optimised for the production of phenylalanine by inducing tryptophan dependency, leveraging the concept of auxotrophy. Auxotrophic mutants are bacteria that cannot synthesise a particular nutrient and are dependent on that nutrient for bacterial growth (Iwasaki et al., 2021). This would make it possible to grow bacteria to a certain OD_{600} until all tryptophan is consumed, after which the pathway would be directed towards production instead of bacterial growth. The nutrient chosen here was tryptophan, which is also known to regulate its synthesis through feedback inhibition by inhibiting the enzyme DAHP synthase, which is involved in the shikimate pathway (Niu et al., 2019). By creating a tryptophan-dependent strain, preferably some of this feedback inhibition would be released, potentially increasing the flux through the pathway that leads to phenylalanine. Two samples of 50 µl of both undiluted and 10-fold diluted bacterial suspension per sample of a strain producing phenylalanine were exposed to UV-C light for 5 and 10 seconds.

Subsequently, these samples were spread on agar plates supplemented with MM and a trace amount of tryptophan (1mg/l), followed by incubation at 30°C. Given the minimal tryptophan content, the assumption was that the larger colonies might not be dependent on tryptophan. Therefore, after a three-day incubation period, 54 smaller colonies were selected and cultured on two distinct agar plates: one without tryptophan and another containing 100 mg/l of tryptophan. The bacteria were cultured on a raster as a method to identify which colonies belong to each other, systematically inoculating the no-tryptophan plate first to eliminate the possibility of growth failure due to the absence of biomass on the inoculation needle. Colonies that did not grow in tryptophan-free medium but did grow in 100 mg/l tryptophan medium were presumed to be tryptophan-dependent and were subsequently cultured in liquid media with (100 mg/l) and without tryptophan to verify this dependency.

2.3.4 Phenylalanine production on differing glucose sources

The phenylalanine-producing strain was tested on MM containing glucose from PC, TC, and WTC being produced in the presence of acetate and phosphate buffer. The goal was to determine whether and to what extent the strain could grow and produce phenylalanine by using the produced glucose as substrate and whether the production differs per substrate. The first batch of glucose sources that were tested were: glucose from PG, TC-AC, WTC-AC, and PC-AC. Before preparation of the medium, the acetate was removed as described in Sec. 2.2.5. The medium was prepared with the same glucose concentrations in conical flasks. The samples were taken at t=0 and inoculated with 100 µl of diluted biomass to an OD of 1.0. At the beginning and end of each day, samples were taken. After taking the samples, the OD_{600} was measured, after which the samples were stored at -20°C for later analysis of the glucose, ammonia, and phenylalanine concentration. After the effect of washing tertiary cellulose before glucose production on fermentation was investigated, a second experiment with different glucose sources was carried out. In this experiment, MM containing PG, G-PC-AC, G-PC-PH, G-TC-AC, G-TC-PH, and G-TC-AH was incubated in duplo with 100 µl diluted biomass of H1 to an OD of 1.0. Again, before preparation of the MM, the acetate was removed from the glucose produced in the presence of an acetate buffer. G-TC-AH also contained a significant amount of acetate, which was removed following the same procedure. Again, a t=0 sample was taken and samples were taken at the beginning and end of each day for three days. OD_{600} was determined after taking the samples and the concentration of ammonium, glucose, and phenylalanine was determined after the experiment at the same time.

3 Results

3.1 Glucose production

3.1.1 Substrate comparison and enzyme optimisation

The efficiency of glucose production from various cellulose substrates was investigated. First, the effectiveness of pure cellulose (PC), tertiary cellulose (TC), and washed tertiary cellulose (WTC) as substrates in the presence of varying enzyme concentrations in acetate buffer was determined with the goal of determining the concentration of cellulose in tertiary cellulose and defining the enzyme concentration.

The yield, or glucose/substrate ratio, was calculated by dividing the amount of glucose produced by the weight of the initial material, adjusting for the water content as shown in Table 2. The yield of glucose from pure cellulose (PC), tertiary cellulose (TC) and washed tertiary cellulose (WTC) with excess enzyme (30%) was 70%, 43%, and 41% respectively (Figs. 5a, 5b, 5c), implying that glucose from TC and WTC yields approximately 60% of the glucose yield from PC. The assumption was made that the rate limiting factor for glucose production from PC is the same in the same order of magnitude for glucose production from TC and WTC. According to this assumption, TC and WTC consist for 60% of cellulose. To start with the same amount of cellulose and compensate for this difference, in subsequent experiments, 40% more TC and WTC relative to PC was used. Furthermore, enzyme concentrations of 13% and 30% resulted in comparable reaction rates and glucose yields, indicating that with 13%, the maximum yield can be approached (Fig. 5d). Consequently, considering the costs of the enzyme, in subsequent experiments, an enzyme concentration of 13% was used.

3.1.2 Normalized glucose production from cellulose

The goal of this experiment was to define whether there are differences in glucose production from the three cellulose substrates (PC, TC, and WTC).

Glucose production in an acetate buffer

In this experiment, the weight of the substrate was normalised based on its defined cellulose content in the previous section to start with the same amount of cellulose, resulting in 60% PC (1.8 g) relative to TC (3 g). The g/c ratio was calculated by the amount of glucose produced over the assumed cellulose weight of the material at t=0 (%, w/w). For TC and WTC, the cellulose fraction was assumed to be 60% of the dry weight of the material. For PC, this was 100% of the dry weight. The g/c ratio profiles from PC (1.8 g), TC (3 g), and WTC (3 g) are similar for the first 72 hours 6. The results after 120 hours were 69, 62, and 48% for PC, TC, and WTC respectively. The decrease in the g/c ratio for WTC after 72 hours could be explained by the consumption of glucose by microorganisms. The reduced yield in glucose production from pure cellulose, compared to the 90% reference in the literature, could be attributed to several factors. The cellulase enzyme's reduced efficacy, potentially due to its age (dating back to 2018), suboptimal stirring conditions, or the crystallinity of cellulose, which could restrict enzyme accessibility. The calculated assumption that 60% of tertiary cellulose is cellulose was based on the yield of pure cellulose; however, the assumption that the factors that lead to the yield of 70% from pure cellulose are identical to those that influence the yields of tertiary cellulose and washed tertiary cellulose may not hold, considering potential alterations in the microcrystalline structures of cellulose throughout the various stages of treatment in the water treatment process.

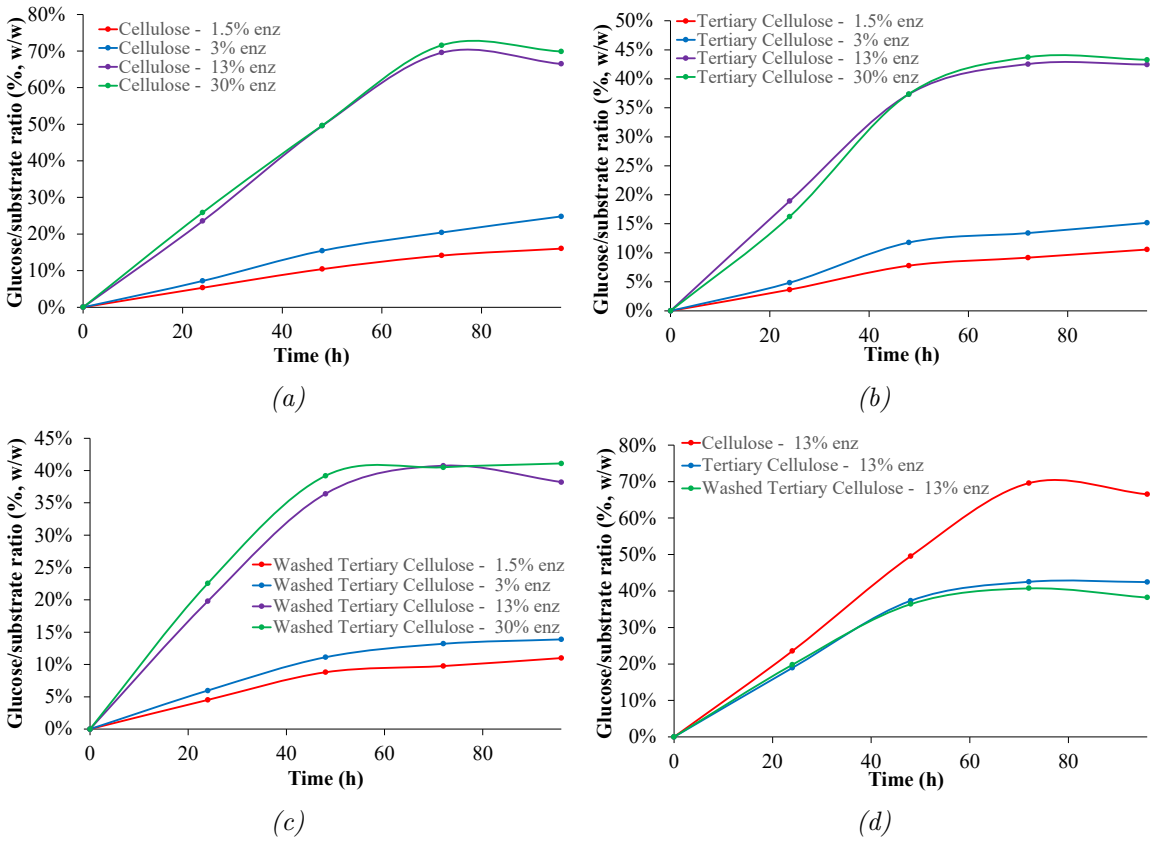

Figure 5: Glucose production with 1.5, 3, 13, and 30% from pure cellulose (a), tertiary cellulose (b), and washed tertiary cellulose (c), and glucose production from the three substrates with 13% enzyme concentration (d)

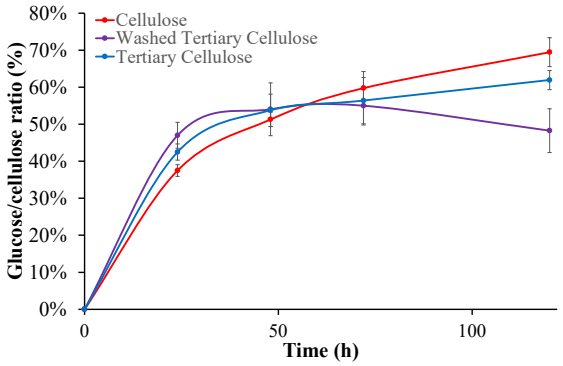

Figure 6: G/c ratio for glucose production in acetate buffer from PC (1.8 g), TC (3 g), and WTC (3 g) with 13% enzyme concentration

Glucose production in a phosphate buffer

The glucose production profile from PC with 13% enzyme concentration was similar to that of TC in a phosphate buffer, with a yield of 88% and 79% after 72 hours for PC and TC

respectively (Fig. 7). Again, in this experiment the weight of the substrate was normalised, resulting in 60% PC (1.8 g) relative to TC (3 g) at t=0. The higher yield observed with the phosphate buffer could be caused by the fact that there could be variations in the cellulose content between different material samples. In addition, the experiments have not been replicated enough to draw hard conclusions.

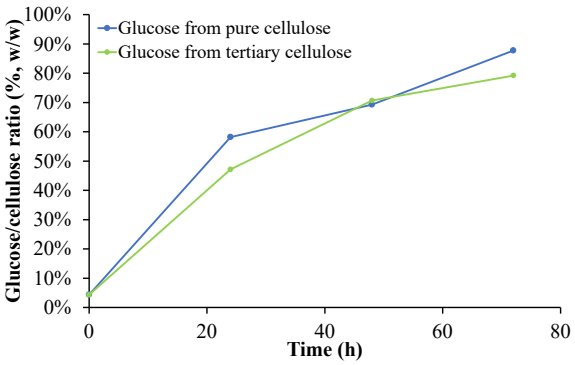

Figure 7: G/c ratio for glucose production in phosphate buffer from PC (1.8 g), TC (3 g), and WTC (3 g) with 13% enzyme concentration

3.1.3 Removal of acetate

Removal of the acetic acid originating from acetate buffer was necessary, as preliminary findings indicated that bacterial growth of *C. glutamicum* was inhibited in a mineral medium containing glucose derived from cellulose hydrolysed in an acetate buffer. The inhibition was attributed to the high residual acetic acid concentration left in the glucose solution, which presented a challenge for the subsequent fermentation process. It was found that a small, undefined amount of phenylalanine and other amino acids was present in the glucose derived from tertiary and washed tertiary cellulose (Fig. 29 in Ap. A). As a result of the presence of amino acids in the glucose derived from TC, acetic acid could not be removed by distillation as the Maillard reaction would be initiated. Therefore, vacuum distillation was performed. and the presence of acetic acid could be demonstrated using the organic acids TLC assay.

Initial trials for acetic acid removal by vacuum distilation were performed on acetic acid in water at 40°C and 50°C (25 mbar). Organic acid TLC analysis (Fig. 8 indicated complete removal of acetic acid after two cycles at 40°C and a single cycle at 50°C. Consequently, subsequent removal of acetic acid from glucose solutions was carried out at 60°C (25 mbar) over three cycles to ensure complete elimination of acetate.

Despite vacuum distillation, the TLC analysis of glucose solutions revealed residual acetic acid (Fig. 9). This presence may be due to precipitation of acetic acid or incomplete evaporation. However, *C. glutamicum* is known to produce small amounts of acetic acid, suggesting that residual levels may not significantly inhibit growth.

Figure 8: TLC organic acids assay showing the removal of acetic acid by vacuum distillation at differing temperatures over several cycles with 5 M (a) and 0.2 M (b) acetic acid, result after vacuum distillation at 40°C after the first (c),second (d), and third (e) cycle, and at 50°C after the first (f), second, (g), third (h) and fourth (i) cycle

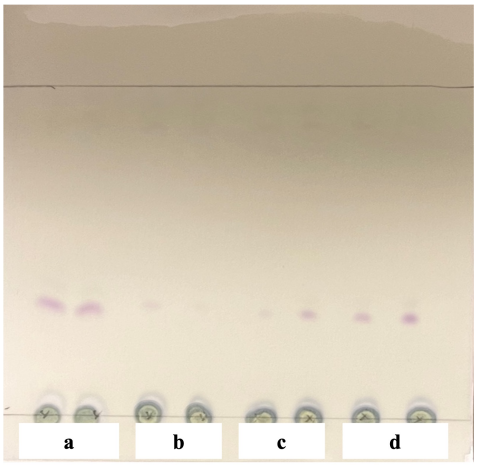

Figure 9: TLC organic acids assay showing the presence of acetic acid in glucose types after vacuum distillation with 0.2 M acetic acid (a), glucose from cellulose (b), tertiary cellulose (c), and washed tertiary cellulose (d)

The TLC organic acids assay was used to detect and quantify acetic acid in MM containing the different glucose solutions. The pH of MM was 7.0, where the acetate buffer had a pH of 5.0. Faint spots suggested the presence of acetic acid residues in MM (Fig. 10). Several dilutions (0, 2, 4, 6, 10, 20) of the acetate buffer were used in order to quantify the removed amount of acetate. The TLC spots increased in size with higher dilutions (Fig. 10), contradicting the expected correlation between concentration and spot size. This indicates that the TLC assay is highly sensitive to pH changes and cannot reliably quantify the presence of acetate in MM with the acetate buffer as a reference. A reason for this inconsistency could be due to the fact that the pH retaining characteristics of the acetate buffer in the sample and the basic buffer

in the assay are working against each other, as a result of which the amidiation step in the assay does not reach full conversion. This was also assumed to be the reason that no visual decrease in acetic acid concentration could be shown for each cycle in Fig. 8.

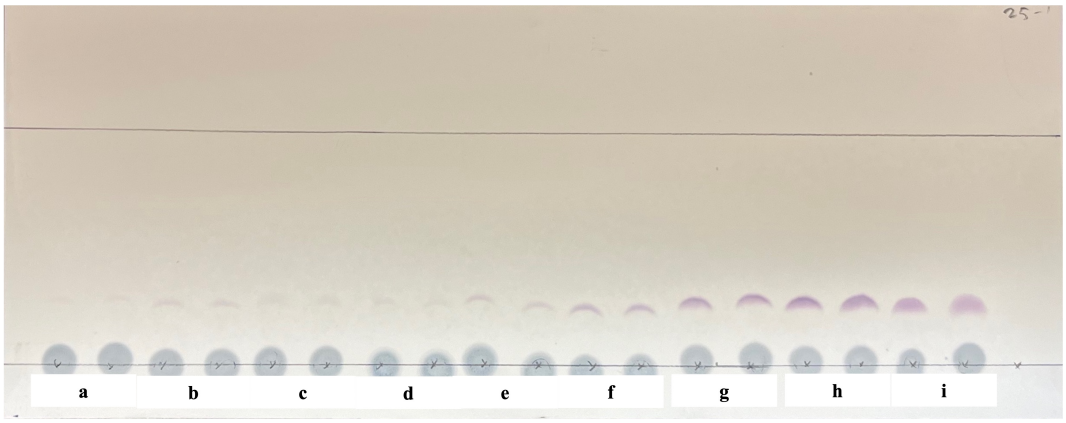

Figure 10: TLC organic acids assay of MM with glucose from cellulose (a), tertiary cellulose (b), acid hydrolysis (c), and from acetic acid buffer being 0(d), 2(e), 4(f), 6(g), 10(h), and 20(i) times diluted

Analysis of impurities

The effect of washing on the presence of impurities was determined at two points: before and after hydrolysis of cellulose.

The weight decrease observed after 14 hours in the drying oven at 60°C was 1%, 4%, and 7% relative to its dry mass for PC, TC, and WTC, respectively. This implies that PC and TC contain 1% and 4% water by weight, respectively, as shown in Table 2. The additional 3% weight loss in WTC is attributed to the removal of soluble impurities along with water by washing. Furthermore, Figure 26 indicates that WTC has more white/grey spots compared to TC, suggesting a difference in residual content after washing.

Table 2: Weight of cellulose types before and after the drying oven

	Before drying (and washing) (g)	After drying (g)	Weight decrease (%)
Cellulose	3.02	2.98	1%
Tertiary cellulose	3.12	3.01	4%
Washed tertiary cellulose	3.04	2.83	7%

To quantify the weight of impurities in the glucose, the theoretical glucose weight (defined by its concentration) was subtracted from the post-vacuum distillation measured weight. It is important to note that the weight difference before and after vacuum distillation encompasses volatile components, potentially including water and volatile organics, but also retains residues like salts and water that has not been evaporated. Hence, the impurity weight ratio calculated—9.7%, 13.9%, and 11.9% for glucose from PC, TC, and WTC respectively (Table 3)—reflects not only organic impurities or acetate precipitates, but also the inherent moisture content and salts, which are not considered impurities per se.

The weights of the non-glucose compounds present in the glucose were quantified by subtracting the theoretical glucose weight defined by its concentration before vacuum distillation from the weight measured after vacuum distillation. The non-glucose ratio was defined by the weight of the non-glucose compounds over the theoretical glucose weight. Non-glucose ratios of 9.7, 13.9, and 11.9% were found for glucose from PC, TC, and WTC respectively (Tab. 3). As PC was assumed to contain no impurities, the 9.7% non-glucose ratio was attributed to water and minor salt precipitates. TC exhibited a 4.2% higher non-glucose ratio attributed to impurities, while WTC showed a reduced excess of only 2.2%, suggesting that washing effectively reduces the impurity weight ratio with 2%.

Table 3: Impurity weight ratio of glucose produced from PC, TC, and WTC

Glucose source	Non-glucose weight ratio (w/w non-glucose/glucose)
Cellulose	9.7%
Tert. cellulose	13.9%
Washed tert. cellulose	11.9%

3.2 Fermentation of glucose from TC in MM for phenylalanine production

The growth characteristics of *C. glutamicum* wild type in MM were assessed by comparing its growth to that in a rich medium (BHI). This comparison aims to evaluate the growth behaviour of the organism in MM, focussing on determining whether this medium provides sufficient nutrients for optimal growth compared to the nutrient-rich conditions in BHI.

The *C. glutamicum* wild type was found to show a longer lag phase in MM compared to BHI, with a max OD_{600} of ∼4.0 after 23 and 43 hours for BHI and MM respectively (Fig. 11). In Fig. 31 (App. A), the bacteria in BHI are shown under a microscope at 1000x magnification.

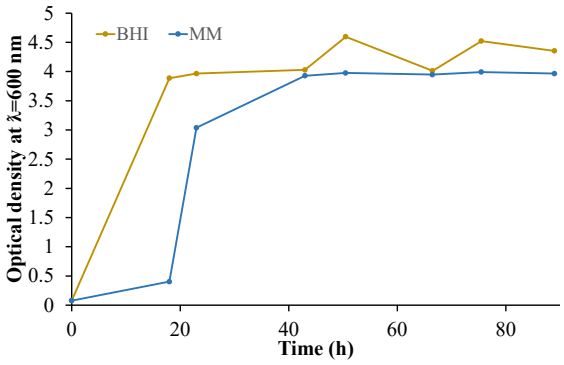

Figure 11: OD600 of C. glutamicum wild type on BHI and MM over time

3.2.1 Incubation in a 96-well microtiter plate for high-throughput screening

Exploring the potential for high-throughput screening, the suitability of using a 96-well microtiter plate for cultivating *C. glutamicum* mutants was evaluated, aiming to streamline the process of identifying high phenylalanine-producing strains. The microtiter plate setup was chosen for its compatibility with spectrophotometric analysis, allowing for continuous

monitoring of bacterial growth at 30°C with periodic shaking overnight. Sterility was maintained through the use of a transparent, adhering lid, which ensured accurate absorption measurements without significant interference. However, challenges with cell sedimentation were encountered, which obscured the spectrophotometric readings. To mitigate this, the medium was diluted four times with sterile water. This dilution facilitated clearer measurements by the spectrophotometer, despite the reduced visibility of growth to the naked eye. Therefore, the set-up relied on the precision of the spectrophotometric readings. A subsequent issue arose with medium condensation forming on the lid, which interfered with the growth measurements. To counter this, the lid was treated with a sterile 1% solution of Triton X-100, rendering it hydrophobic and preventing the accumulation of condensate. After several experiments, none of the inoculated strains exhibited growth, possibly due to the excessive dilution of the medium. Consequently, the decision was made to discontinue the use of the 96-well microtiter plate approach, as optimising the conditions proved time consuming and was detracting from the primary research focus.

3.3 Generation of a *C.glutamicum* mutant with high phenylalanine production potential by random mutagenesis

As *C. glutamicum* DSM20300 did not naturally produce phenylalanine, it was randomly mutated to redirect its metabolic pathway towards enhanced phenylalanine production via the shikimate pathway.

Effects of F-phenylalanine on bacterial growth

To define the MIT (minimal inhibitory concentration) of F-phenylalanine for *C. glutamicum* growth, bacteria were grown in MM with various concentrations of F-phenylalanine. F-phenylalanine appeared to significantly reduce *C. glutamicum* growth at 25µg/ml, with increased inhibition at higher concentrations (50, 100, 500, 1000, and 2000 µg/ml), even though the optical densities are similar after 46 hours (Fig. 12). In the TLC amino acids assay conducted from the media after 46 hours, the different F-phenylalanine concentrations can be seen, with no significant changes in production (Fig. 32 in Ap. A).

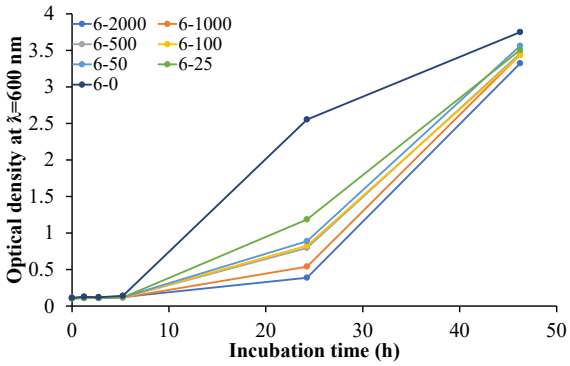

Figure 12: OD600 of C. glutamicum on MM with 0, 25, 50, 100, 500, 1000, and 2000 µg/ml analog over 46 hours

To identify the source of the MM dot in Fig. 32 (Ap. A), a TLC amino acid assay was performed with its components. The assay indicates that the MM spot originates from ammonium chloride and magnesium sulphate (Fig. 13).

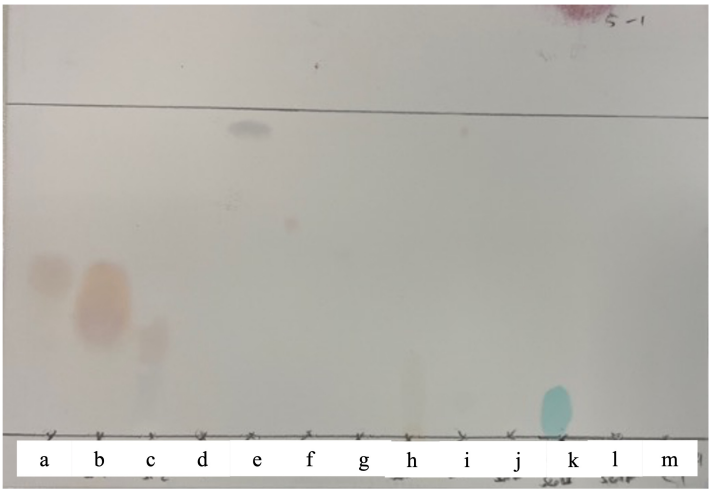

Figure 13: TLC amino acid assay with mineral medium and its components from left to right: a:MM, b:NH_4Cl & $MgSO_4 * 7H_2O$, c:KH_2PO_4&K_2HPO_4, d:D-glucose, e:PCA, f:Biotin, g:CaCl, h:$FeSO_4 * 7H_2O$, i:Trace elements, j:$MnSO_4 * 7H_2O$, k:$CuSO_4$, l:$ZnSO_4 * 7H_2O$, m:$NiCl_2 * 6H_2O$

3.3.1 UV mutagenesis

No growth was observed on agar plates containing 25 and 50 µg/ml analogue with 100 µl x1000 and x100 dilution and UV-C exposure of 15, 30, 45, and 60 seconds after seven days in an incubator at 30°C (Tabs. 9 & 10 in Ap. B). As finding the working combination between the analogue concentration, inoculum dilution, and UV-C exposure time was found to be time-consuming, it was decided to perform UV mutagenesis on liquid cultures, followed by growth in liquid media. This approach was expected to enhance the efficiency of selecting phenylalanine-producing strains because of the increased competitive selection pressure, potentially accelerating the isolation of a high-yielding phenylalanine-producing strain.

In liquid mutagenesis, growth occurred in instances where 50µl samples without dilution were subjected to UV-C for 15 seconds with 25 (7-25-15) & 50 (7-50-15) µg/ml analogue in conical flasks. No growth was observed for 30 and 60 seconds of exposure to UV-C (Tab. 11). A significant amount of phenylalanine was found to be produced in the sample exposed to UV-C for 15 seconds in the presence of 25µg/ml analogue (Fig. 14). No significant phenylalanine production was observed with 15 seconds UV-C exposure in 50µg/ml analogue. As the analogueue and phenylalanine have almost the same Rf value, a dot volume analysis was performed that supports these findings with an increase in dot volume of 41.9 for the 25µg/ml analog, and a minor increase of 9.5 for the 50µg/ml analog (Tab. 4). The blue dots on the TLC sheet are formed by the ink of a ballpoint pen. It should be noted that afterward, it was hypothesised that the light had to warm up until it will emit a consistent and reproducible amount of light. Therefore, the exposure time after which the colonies mutated and survived might not be reproducible.

The isolation of mutants present in 7-25-15 from agar plates containing different concentrations of F-phenylalanine resulted in isolated colonies in MM with various production profiles after three days of incubation (Fig. 35 in Ap. A). Analysis of the dot volumes of all isolated phenylalanine-producing mutants (Fig. 15) showed that the production of phenylalanine for

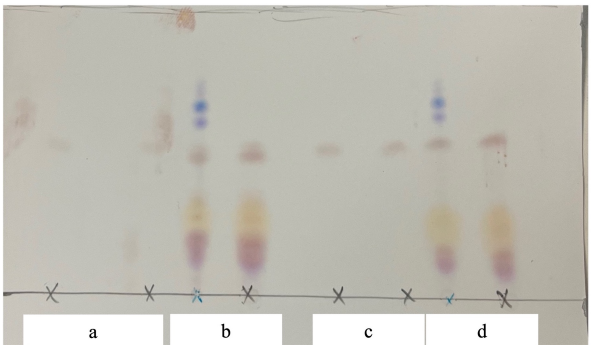

Figure 14: TLC amino acids assay of 25 (a) and 50 (c) µg/ml F-phenylalanine, and after 15 seconds UV mutagenesis and growth in MM in the presence of 25 (b) or 50 (d) µg/ml F-phenylalanine

Table 4: Dot volumes of (F-)phenylalanine dots after mutagenesis

	Dot volume
F-phen (25 µg/ml)	11.7
7-25-15	53.6
F-phen (50 µg/ml)	23.0
7-50-15	32.5

all mutants was lower than 0.25 g/l, as their dot volume (max. 12.8) was significantly lower than the dot volume of 0.25 g/l phenylalanine (23.4) (Tab. 12 in Ap. B). Isolated mutants C1 & C4, with dot volumes of 10.8 & 12.8 respectively were chosen for further mutagenesis based on their relatively high dot volume. The OD_{600} of the isolated strains was not measured.

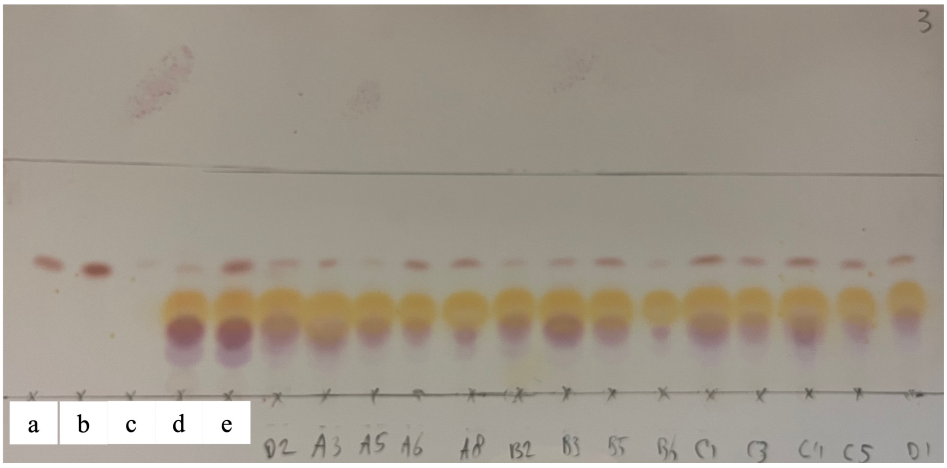

Figure 15: TLC amino acids assay with 0.25 (a) and 0.5 (b) g/l phenylaline, 25 µg/ml F-phenylalanine (c), the mutated strain being isolated (7-25-15) without (d) and with 25 µg/ml F-phanylalanine, and phenylalanine-producing strains after isolation of the first phenylalanine-producing mutant in MM in the absence of F-phenylalanine

A second liquid mutagenesis was performed with strains C1 and C4 with several combinations

of UV-C exposure (5, 10, 15, 20 sec.) and analogue concentration (50, 100, 200 µg/ml) (Fig. 16). As the analysis of the production improvement in comparison with C1 & C4 should be defined by the dot volume of the mutant minus the dot volume of C1/C4 and the analogue, it was too dependent on the precision of the pipets, assay, and quantification tool. Therefore, it was decided to isolate the best two mutants for each concentration of analogue based on its exposure time, dot volume, and OD_{600}. The strains chosen to isolate were C4-10-50, C1-20-50, C4-5-100, C4-10-100, C1-15-200, and C1-5-200 with dot volumes of 12.6, 10.1, 15.5, 15.3, 19.5, and 19.6 respectively (Tab. 13 in Ap. B). The OD_{600} of the mutants did not vary significantly for these strains and therefore was not taken into account in the decision for this selection.

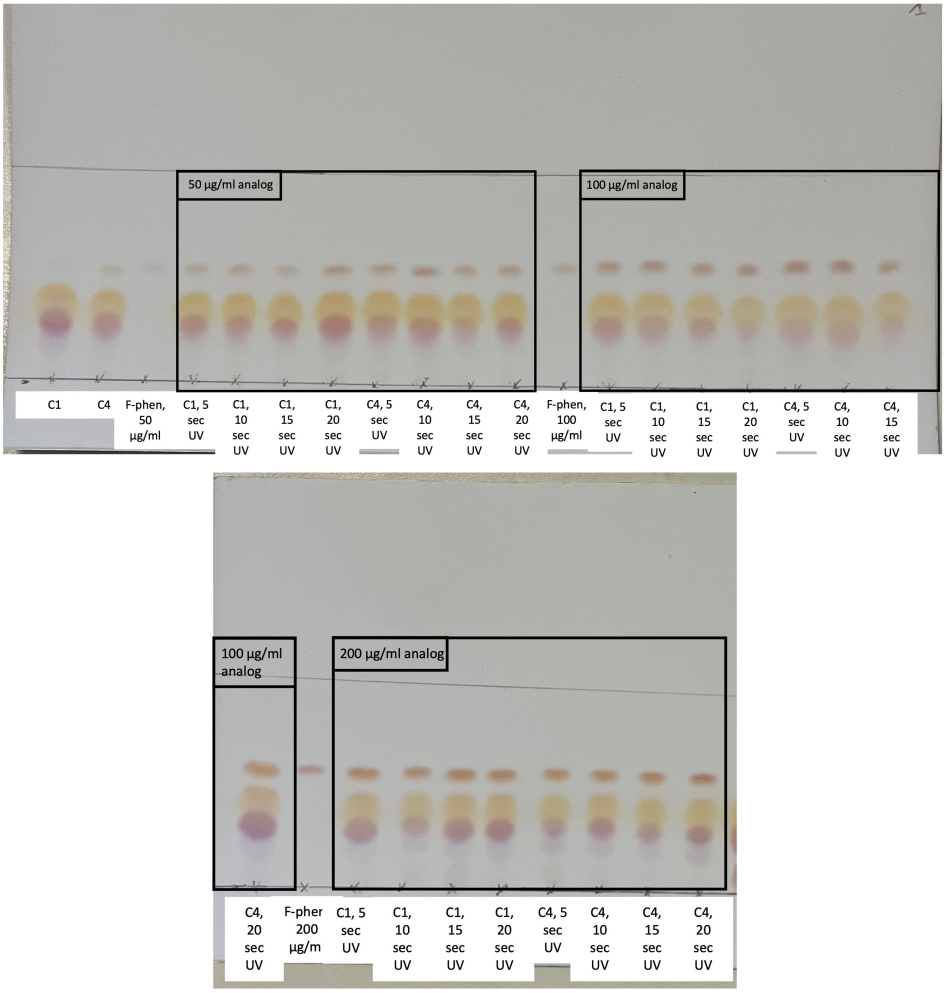

Figure 16: TLC amino acids assay after growth in MM containing 50, 100, and 200 µg/ml F-phenylalanine after UV-C exposure times of 5, 10, 15, and 20 seconds on C1 and C4 strains of previous isolation

The isolation of mutants was done on agar plates with MM and several concentrations of analogue, depending on their analog concentration in their previous medium with x10 and x100 dilutions on each plate (Fig. 34 in Ap. A). TLC amino acid assay of isolated strains showed phenylalanine production for all growth samples (Fig. 36 in Ap. A). Dot volume

analysis did not show phenylalanine production higher than 0.25 g/l, and the highest dot volume for G2 with a dot volume of 28.32 and an OD_{600} of 2.48 (Tab. 14 in Ap. B). As only visual assessment and not software was used at the moment of measurement, H1 was assigned for further experiments based on its visually high spot density. Glycerol stocks of F7, F8, F9, F11, H1, H2, H5, H6, H8, H9 were stored at -80°C.

Engineering of a tryptophan-dependent phenylalanine-producing strain
Isolation of 54 mutants after 5 & 10 seconds UV-C exposure of H1 on agar plates containing 1 mg/l tryptophan to agar plates containing 0 % 100 mg/l tryptophan resulted in two mutants growing on the plate containing 100 mg/l, and not growing on the plate without tryptophan. This would imply that eventually the phenylalanine-producing strain would be tryptophan dependent. However, in contrast to this conclusion, the isolation of the two colonies in liquid MM with 0 and 100 mg/l tryptophan, showed growth in both media (Fig. 17).

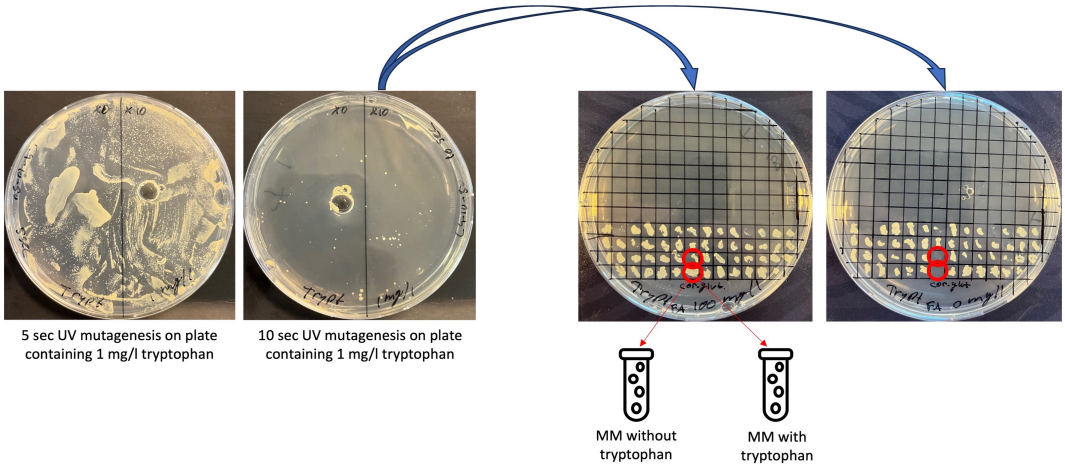

Figure 17: Agar plates showing the results of mutagenesis and isolation of strains to mutate and isolate a tryptophan-dependent strain

3.3.2 Production of phenylalanine by H1 from MM containing G-PC-AC, G-TC-AC, and G-WTC-AC

Analysis of the concentration of phenylalanine during H1 growth in MM with different glucose sources produced in the presence of acetate buffer showed a similar production rate, whereas production from PC lags in production for the first 17 hours. A final phenylalanine concentration of 0.47, 0.52, and 0.71 g/l was obtained when growing in MM with PC, TC, and WTC respectively. The glucose consumption rate corresponded to the increase of the OD_{600} growth curve, where MM with G-PC showed a longer lag phase in both graphs. The observed glucose levels of 1.0, 1.7, and 1.0 g/L after 72 hours for PC, TC and WTC respectively confirm that glucose is the reaction-limiting component. The visible decrease in ammonia concentration is not assumed to be assigned to phenylalanine production but mainly to biomass production. This, as theoretically, for the end concentrations of phenylalanine obtained, only a decrease of 0.049, 0.054, and 0.073 g/l ammonia could be assigned to phenylalanine production from PC, TC, and WTC respectively. Due to the small decrease in concentration, ammonium was not found to be the reaction-limiting component (Fig. 18). The differences observed in the experiments were not statistically significant, considering the standard deviation. The

insignificance for phenylalanine production could be due to the inaccuracy in determining the phenylalanine concentration by defining the dot volume on TLC. Efforts were made for HPLC analysis, however technical constraints limited this feasibility.

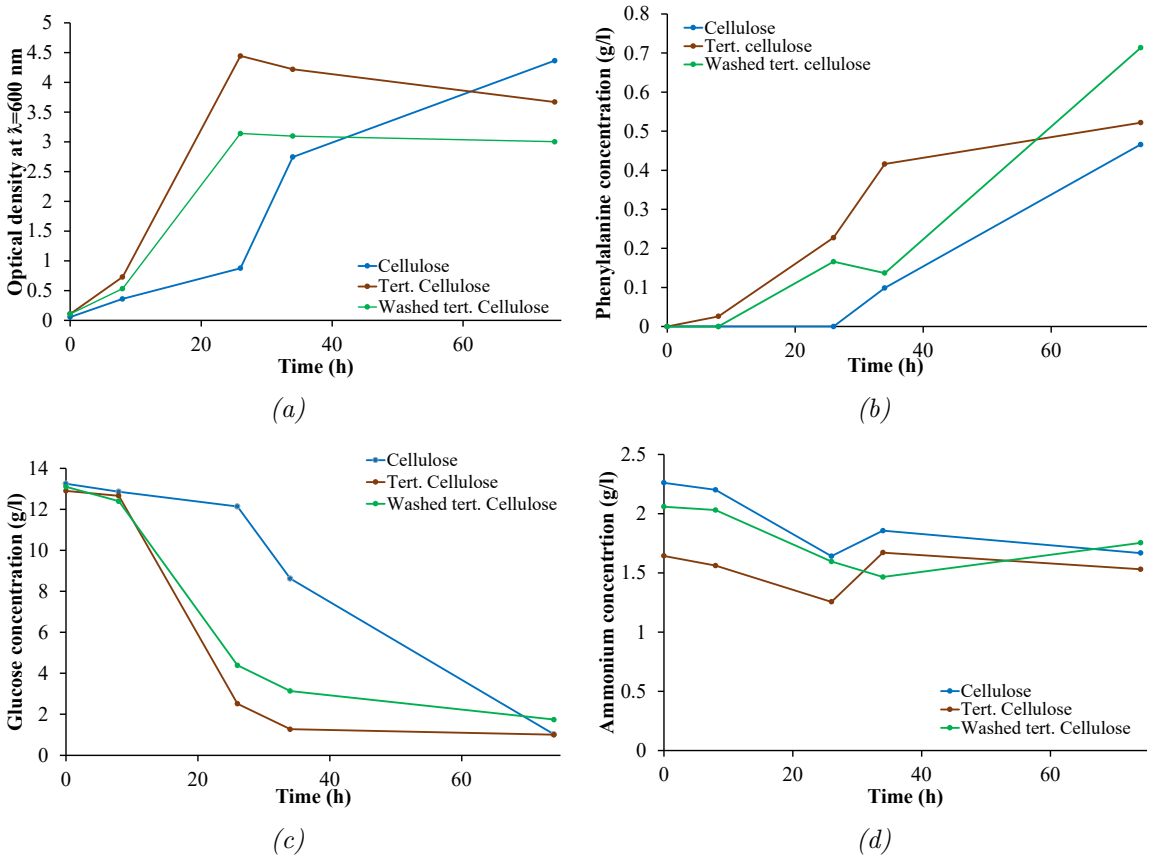

Figure 18: Graphs of OD_{600} (a), phenylalanine production (b), glucose consumption (c) and ammonium concentration (d) over time on mineral medium with glucose produced from pure, tertiary, and washed tertiary cellulose

3.3.3 Production of phenylalanine by H1 from MM containing G-TC-AC, G-PC-AC, G-TC-PH, G-PC-PH, and G-TC-AH

Similar slopes were observed for all samples with MM containing G-PC, G-TC, and G-TC-AH for OD_{600}, phenylalanine production, glucose consumption, and ammonia consumption. The higher OD_{600} of the samples containing G-PC in acetic acid buffer could be explained by its higher glucose concentration at t=0. As in Fig. 18, glucose, and not ammonia was found to be the reaction-limiting component. The growth of glucose produced in the presence of the acetate buffer confirmed the successful removal of enough acetate to prevent growth inhibition. Average phenylalanine concentrations were obtained after 64 hours of 0.39, 0.57, 0.42, 0.25, and 0.55 g/l for MM containing G-TC-AC, G-PC-AC, G-TC-PH, G-PC-PH, and G-TC-AH (Fig. 19). The phenylalanine production did not stop increasing visibly, suggesting that monitoring for an extended period could reveal a higher phenylalanine production, possibly due to the presence of intermediate metabolites still undergoing conversion to phenylalanine even after glucose depletion.

During the two experiments in this section, four attempts were made to monitor the growth,

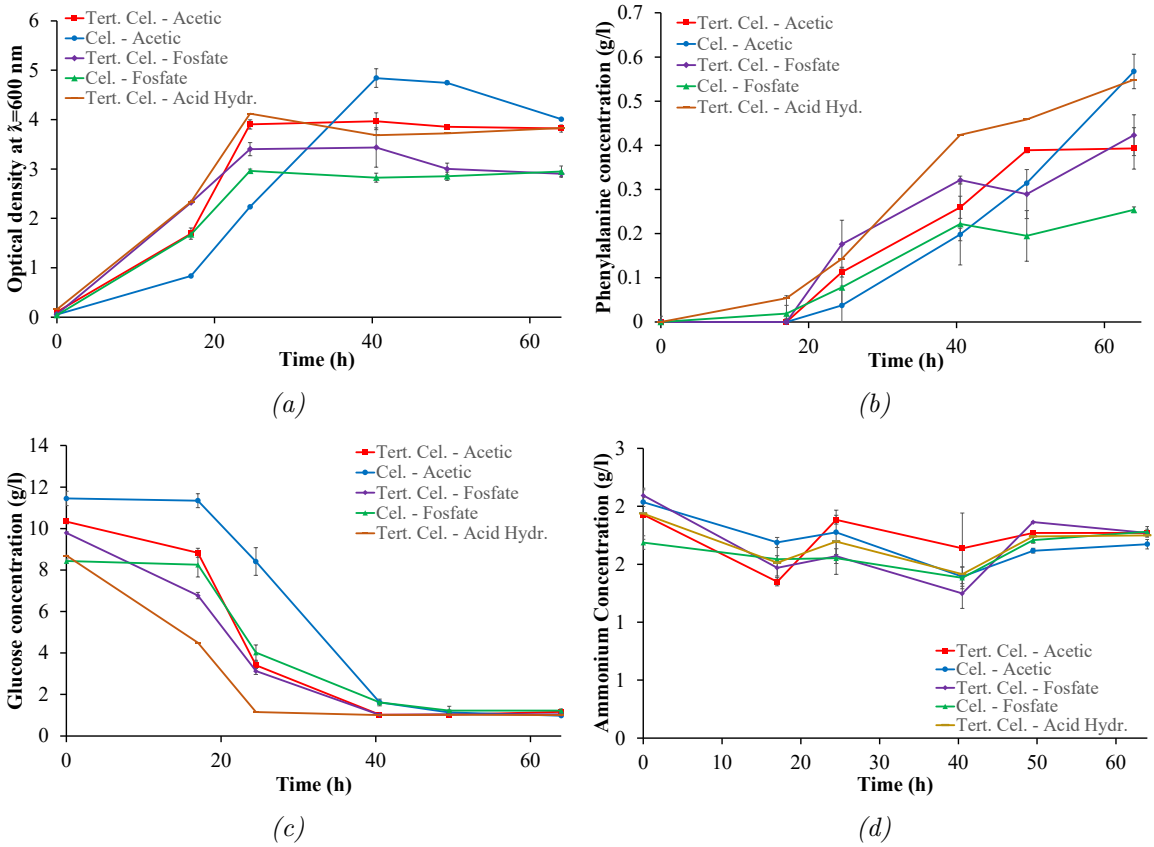

Figure 19: Graphs of OD_{600} (a), phenylalanine production (b), glucose consumption (c) and ammonium concentration (d) over time on mineral medium with glucose produced from pure and tertiary cellulose on in the presence of an acetate and phosphate buffer, and glucose produced by acid hydrolysis

production, and consumption of H1 in MM with pure glucose. During these experiments, no growth or production was observed. As H1 did grow on the other glucose sources, and no growth was observed in negative controls, the strain was tested by inoculating it in a rich medium (BHI), resulting in a normal growth curve. To test whether the cause lay at the MM, *C. glutamicum* DSM 20 300 wild type was inoculated in the MM, resulting in a maximum OD of 1.43 after four days, in contrast to the maximum OD of 4.0 reached in previous experiments (Fig. 11). This difference suggests that something has changed in the state or presence of components in MM, resulting in no growth of H1 with pure glucose, but not limiting growth on MM with other glucose sources to grow. Suggesting that other glucose sources might contain this/these component(s).

Based on the fact that glucose seems to be the reaction-limiting component in the previous graphs, fed-batch was found promising. This was executed on MM with pure glucose, which showed an increase in production after glucose addition, but stabilised at a maximum end concentration of 0.46 g/l phenylalanine after 9 days, which was not significantly higher than the production from alternative glucose sources in Figs. 18 & 19. This experiment was carried out earlier with a different MM source that seemed to work, but it cannot be ruled out that

the reason for the low production is the same as the reason for no growth on MM with PG.

3.4 Identification of side products

Earlier TLC analyses led to the hypothesis that the yellow dot with an Rf of $\sim$ 0.42 was glutamate. Lysine and tryptophan were not produced. Other amino acids (aspartate, glutamic acid, methionine, aspartic acid, glutamine, and arginine) were spotted next to growth of H1 over time to hypothesise whether and if other amino acids formed (Fig. 20). Side products tend to vary for MM containing differing glucose sources (Figs. 37-41 in Ap. A). Comparing the Rf values of the amino acids standard in Fig. 20 with the production profiles in Fig. 37-41, led to the hypothesis that aspartate and glutamic acid might be produced. Another hypothesis is the production of tyrosine, as this is produced via the shikimate pathway. This should be confirmed with HPLC, but could not be executed for technical reasons.

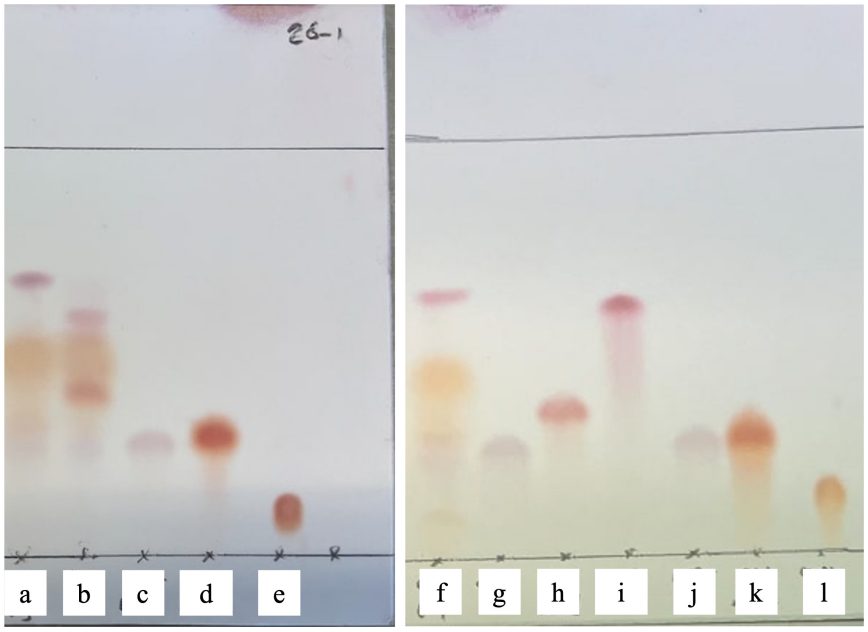

Figure 20: TLC amino acid assay showing phenylalanine production on glucose from acid hydrolysis (a), amino acid production by wildtype (b), aspartate (c), glutamine (d), lysine (e), production after growth on glucose from pure cellulose (f), aspartate (g), glutamic acid (h), metionine (i), aspartic acid (j), glutamine (k), and arginine (l)

4 Economic Feasibility on an industrial scale

After the technical feasibility of the production of phenylalanine from tertiary cellulose was confirmed, the potential of the process for execution on an industrial scale was evaluated.

The process was divided into three parts: retrieval of tertiary cellulose from the wastewater treatment plant (WWTP), glucose production by either acid (route 1) or enzymatic (route 2) hydrolysis, and fermentation of glucose for the production of phenylalanine using *C. glutamicum* (Fig. 21). Here, since enzymes are known to be expensive, route 2 assumes the production of cellulase by *Trichoderma reesei*. For all models, an electricity price of 0.085 $/kWh was used, in line with the current wholesale price of electricity in the Netherlands (78.4 euro/MWh) (Statista, 2024).

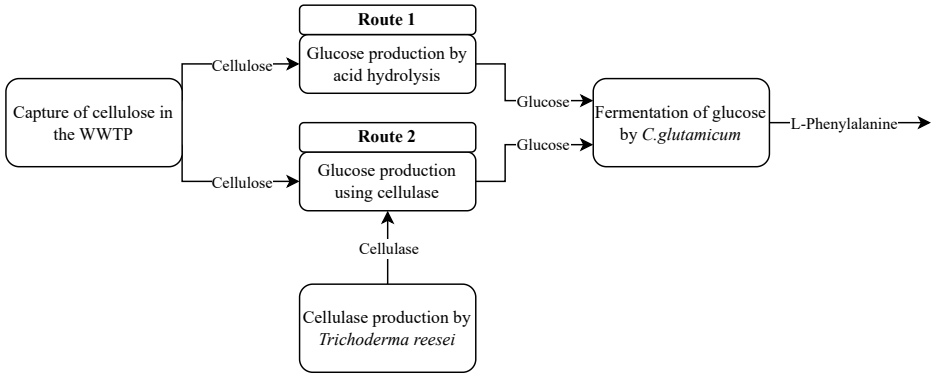

Figure 21: Production of phenylalanine from tertiary cellulose via two routes: enzymatic hydrolysis and acid hydrolysis of cellulose

As the required production scale of the three processes is highly dependent on the desired output of phenylalanine, the processes are explained beginning with the fermentation.

4.1 Production of phenylalanine from glucose by fermentation

Production of phenylalanine from glucose was done via the shikimate pathway by fermentation of *C. glutlamicum*. To model the process, a fermentation model provided by Intelligen, Inc. was used and adapted for the production of phenylalanine, leading to an annual production rate of ∼8,000 ton phenylalanine per year. The required amount of glucose for this production scale is expected to be 55,845 tons of glucose per year. The process was divided into four parts: fermentation, harvest, chromatography, and crystallisation and recovery (Fig. 42-45 in Ap. C).

4.1.1 Fermentation

Fermentation was carried out at 32°C, starting with two seed fermenters P-01 and P-05 with a volume of 2.05 and 40.55 m^3 and a reaction time of 20 and 36 hours, respectively. After seed fermentation, the main fermenter (P-06) is filled with sterile media and broth. The main fermenter has a volume of 458 m^3 and is operated for 42 hours (Fig. 42 in Ap. C). Based on several sources that confirm the successful production of ∼20 g/l phenylalanine by fermentation of glucose using *C. glutamicum*, the stoichiometric mass coefficients in Eq. 1 were designed (Ikeda et al., 1993),(Pérez-Sánchez et al., 2021). In Eq. 1, SH and OA stand for soy hydrolysate and organic acids respectively. An assumed conversion of 99% led to an

achieved target concentration of 20.15 g/l phenylalanine.

$$22NH_3{+}207\,\text{Gluc.}{+}150O_2{+}16\,\text{SH} \Rightarrow 53.25\,\text{Biom.}{+}178.25CO_2{+}27.25\,\text{OA}{+}28\,\text{Phen.}{+}108.25H_2O \quad (1)$$

4.1.2 Harvesting

After fermentation, the fermentation broth is centrifuged to separate biomass from the supernatant. Subsequently, the supernatant is treated with sulfuric acid for the synthesis of phenylalanine sulphate (Fig. 43 in Ap. C). The biomass obtained by centrifugation is dried and valued at $200 per ton as an animal feed ingredient due to its nutritional value.

4.1.3 Chromatography

In the chromatography process, a cation exchange column is utilised to separate phenylalanine from other organic acids and impurities, capturing 96% of the phenylalanine content. This high level of efficiency is achieved by first adjusting the pH of the phenylalanine sulphate solution to a lower value. This adjustment ensures that the phenylalanine molecules are positively charged, allowing them to bind effectively to the negatively charged resin of the cation-exchange column, while the sulphate ions, which are negatively charged, are not retained by the resin.

After the phenylalanine molecules are adsorbed onto the resin, they are eluted using an ammonium hydroxide solution. This elution process releases the phenylalanine from the column, and it is then collected in a buffer tank, ready for the subsequent crystallisation stage (Fig. 44 in Ap. C).

4.1.4 Crystallisation

The amino acid solution in the phenylalanine buffer tank, containing ammonium hydroxide, is first acidified using sulfuric acid. This step helps to retain ammonia in the solution by converting it to ammonium sulphate, preventing its evaporation during subsequent processes. Following acidification, the solution is concentrated by evaporation, cooled, and then transferred to a crystallisation tank. In this tank, additional HCl is added to neutralise the ammonium hydroxide (Eq. 2), resulting in the formation of phenylalanine HCl through a reaction with HCl (Eq. 3). After the mixture is cooled to (15°C), it is assumed that 98% of phenylalanine HCl crystallises, which can then be separated from ammonium chloride by centrifugation.

Crystallised phenylalanine HCl was redissolved in an aqueous solution of ammonium hydroxide to neutralise any excess HCl, followed by purification in an activated carbon unit. This unit effectively removes most residual organic acids and decolorises the solution. Subsequently, the purified phenylalanine solution is transferred to a second crystallisation tank, maintained under the same conditions as the first, to induce further crystallisation. The final product is then filtered, washed and dried (Fig. 45 in Ap. C), resulting in phenylalanine HCl with an assumed purity of 99.8%.

$$1HCl + 1NH_4OH \Rightarrow 1NH_4Cl + 1H_2O \quad (2)$$

$$1HCl + 1\,\text{Phenylalanine} \Rightarrow 1\,\text{Phenylalanine-}\,HCl \quad (3)$$

4.2 Production of glucose from cellulose by acid hydrolysis

As calculated by using the superpro model for the production of 8,000 tons of phenylalanine per year, the required glucose production was 55,845 tons/year. The process of producing glucose from tertiary cellulose by acid hydrolysis involves a reactor, followed by a centrifuge that removes unreacted cellulose and a column of phenylboronic acid to isolate glucose from sulfuric acid and inhibiting byproducts (Fig. 22). The reaction was assumed to proceed according to the optimal reaction conditions defined by Morales-delaRosa et al., where a glucose yield of 20% was obtained by acid hydrolysis with a sulfuric acid concentration between 0.2-0.5 mol/l at 140°C for two hours following the mass stoichiometry shown in Eq. 4. For the model, a sulfuric acid concentration of 0.35 mol/l was assumed. As the glucose yield was assumed to be 20%, and the amount of cellulose in tertiary cellulose was found to be ∼60%, a glucose yield of 12% is expected from tertiary cellulose. With this information, 465,375 tons of tertiary cellulose are required each year to meet the yearly required amount of glucose.

$$1\,(\text{cellulose})_n + (n-1)\,\text{H}_2\text{O} \rightarrow n\,\text{glucose} \tag{4}$$

The water content in tertiary cellulose is expected to be 5g/g glucose (elaborated on in sec. 4.4). To ensure a good mixing in the reactor, the reactor will be filled with water until a water content of 7 g/g glucose has been reached. This is less than in the experiments with the tube rotator (15 g water/g glucose), but as a mixer is assumed to have a higher mixing efficiency, a lower amount of water is assumed to be needed. A volume of tertiary cellulose of 1.33 ml/g was assumed, calculated based on the information that the tubes containing 45 ml buffer were filled to 49 ml with 3 grammes of tertiary cellulose.

Assuming 330 operating days per year and a batch time of 4 hours for the reactor, the decision was made for the operation of three sequential reactors producing a total of 1,980 batches per year. Using the data provided, it was defined that with a maximum filled reactor percentage of 90%, the required reactor size for the three reactors should be 135m^3. Reactor costs for this scale for a carbon steel reactor with a design temperature of 340°C were estimated to be ∼50,000 $ per reactor in 2002 (Loh et al., 2002). To account for inflation and changing market conditions, the Chemical Engineering Plant Cost Index (CEPCI) was used to adjust this cost estimate for 2002 to a value for 2024. The CEPCI tracks cost changes specifically relevant to chemical process plants. Applying the ratio of the CEPCI in 2024 (295.6) to the CEPCI in 2002 (128.7), the estimated reactor cost in 2024 were determined to be approximately $115,000 (Skills, 2024). The centrifuge cost were estimated to be $242,000 using the same inflation correction for the price (Loh et al., 2002). Following the centrifuge, the resulting product stream contains glucose along with sulfuric acid and various by-products (including levulinic acid). As sulfuric acid and by-products are expected to inhibit growth during the fermentation step, glucose must be isolated. To isolate the glucose, a phenylboronic acid (PBA) column will be employed. PBA has a specific affinity for compounds containing cis-diol groups, such as glucose (Wu et al., 2016). This allows the column to selectively retain glucose while sulfuric acid and by-products lacking the diol structure pass through. The bound glucose can then be recovered by elution with a solution that disrupts the PBA-glucose interaction. For the model, a sodium hydroxide solution was used as a solvent, which has to be mixed with hydrochloric acid to produce NaCl before fermentation. This part was not included in the model. Material costs for the PBA column are expected to be $165,000, consistent with one-third of the price for the column in the SuperPro phenylalanine production model, as the required volume is also

one-third of the volume in the phenylalanine model. Although this represents a significant investment, the separation is essential to obtain a glucose stream suitable for subsequent purification and use in phenylalanine synthesis. Additionally, the disposal of sulfuric acid and by-products will incur costs. As a result of the complex mixture of byproducts, recovery of ammonium sulphate is not considered feasible for sale as a fertiliser. Instead, disposal costs of approximately \$1/tonne will be incurred.

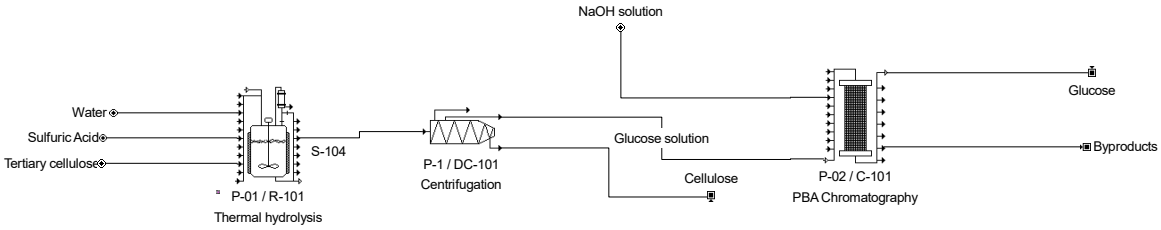

Figure 22: Superpro model for glucose production by acid hydrolysis of tertiary cellulose

4.3 Production of glucose from cellulose by enzymatic hydrolysis

The production of glucose by enzymatic hydrolysis of cellulase involves the reaction in a reactor (Eq. 4), after which the glucose mixture is centrifuged. Subsequently, acetic acid and water are evaporated by vacuum distillation (Fig. 23). Based on the assumed glucose yield of 90% from pure cellulose (Hall et al., 2010), and the assumption that 60% of the tertiary cellulose consists of cellulose, a glucose yield from tertiary cellulose of 54% is expected. Based on this yield, yearly 103,417 tons of tertiary cellulose is needed to meet the required amount of glucose of 55,845 tons/year. A batch time of 72 hours was assigned to the process, of which 48 hours involved the enzymatic hydrolysis reaction executed at 50°C. To maintain pH at 5.0, the acetate buffer containing 0.2 M acetic acid and 0.35 M sodium acetate was used. The selection of acetate buffer over phosphate buffer was based on energy considerations. Utilising phosphate buffer requires sterile conditions to prevent microbial consumption of glucose, which requires all materials to undergo sterilisation at 121°C for 15 minutes. On the contrary, the acetate buffer, although it requires posthydrolysis removal, is expected to be more energy efficient, as the removal process is feasible at a lower temperature of 60°C. Also, unlike the phosphate buffer where pre-heating the entire substrate is mandatory, the acetate in the acetate buffer is evaporated after the removal of the cellulose and impurities, minimising the amount of chemicals to be heated. As the reactor is used at standard pressure, a relatively neutral pH of 5.0, and a temperature of 50°C, the material requirements are expected to be significantly lower, decreasing the reactor costs. Therefore, the reactor costs were estimated to be the same (\$115,000) for a reactor that has double the volume (270 m^3). It was decided to use six sequential reactors of (270 m^3) to meet the required annual glucose production. Centrifuge costs were estimated to be the same as for acid hydrolysis (\$242,000). The distillation column was estimated at \$460,000 after correcting for the time difference by applying the CEPCI ratio.

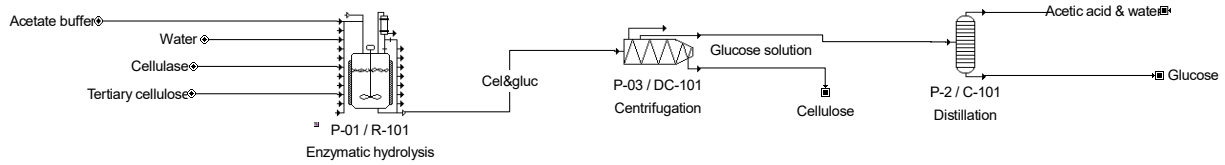

Figure 23: Superpro model for glucose production by enzymatic hydrolysis of tertiary cellulose

Production of cellulase by *Trichoderma reesei*
As cellulase costs are known to be expensive (45-60$/kg), in this case, it is assumed that cellulase is produced using *Trichoderma Reesei*. The process has been modelled in SuperPro by Taiwo et al.. It was found that cellulase could be produced in semi-batch for 22.12 $/kg on a production scale of 1371 tonnes of dry cellulase per year. As for the production scale in this model, only 277 tons of dry cellulase are needed, the price is expected to be higher for production on this smaller scale. However, as glucose is used as the carbon source for fermentation and is known to account for a significant amount of the raw material costs in fermentation, it is assumed that the glucose produced can be used for this process, lowering the cellulase price and compensating for the lower economy of scale.

4.4 Retrieval of tertiary cellulose from the WWTP

The process of recovering tertiary cellulose involves only the use of screens able to filter the incoming feed in a WWTP for particles with a particle size high enough for cellulose. The tertiary cellulose does not have to be dried, as during hydrolysis less water has to be added. To determine the amount of water to add during cellulase hydrolysis, it was assumed that the tertiary cellulose contained 5 grammes of water per gramme of tertiary cellulose. Capital costs involve only cellulose screens, with an estimated price of €185,000 for a screen with a capacity of 500m^3/h and a scale factor of 0.75 (Khan et al., 2022). Operational expenditures are expected to be power, estimated at 34.6 kW for a base case capable of processing a wastewater flow of 540m^3/h containing 75 kg of dry matter per hour.

The total dissolved solid concentration of domestic wastewater ranges between 250-850 mg/l (Park and Snyder, 2020). The cellulose screens in this case filter solid particles starting from the cellulose particle size, while succeeding in capturing more than 80% of the influent cellulose (Ahmed et al., 2019). As it was found that 540m^3 wastewater contains 75 kg tertiary cellulose, the yearly amount of wastewater required for the production of 8,000 tonne of phenylalanine was found to be 3,351 and 745 million m^3 for acid and enzymatic hydrolysis, respectively. These volumes comply with the wastewater of approximately 71 and 16 million people for acid and enzymatic hydrolysis, respectively.

4.5 Production costs

Using the information provided in Sec. 4.4, and an estimated plant lifetime of 30 years, the tertiary cellulose retrieval costs per kg are 0.0020 and 0.0029 for the acid and enzymatic hydrolysis scale, respectively. The CAPEX were determined using the scale factor of 0.75, where the OPEX were assumed to have a linear relation with scale, as the only OPEX was assumed to be electricity. Total annual retrieval costs for acid and enzymatic hydrolysis were found to be 915,498 and 296,077 €/year, respectively, to meet the glucose demand for the defined production scale for phenylalanine. The prices for cellulose retrieval are defined in

euros as the information from the sources was in euros. Other prices later in the report are shown in dollars, as Superpro was programmed for dollars 5.

Table 5: Calculation of CAPEX, OPEX, and costs per kg of tertiary cellulose retrieval for the acid and enzymatic hydrolysis route

Retrieval of tertiary cellulose by acid hydrolysis of cellulose		
Required amount of tertiary cellulose	465,375	tonne/year
Cost-scaling factor	148	
CAPEX	27,395,812	€
OPEX	2304	€/year
Total costs	915,498	€/year
Costs per kg	0.0020	€/kg
Retrieval of tertiary cellulose by enzymatic hydrolysis of cellulose		
Required amount of tertiary cellulose	103,417	tonne/year
Cost-scaling factor	48	
CAPEX	8,866,961	€
OPEX	512	€/year
Total costs	296,077	€/year
Costs per kg	0.0029	€/kg

Using the defined cellulose costs, the glucose costs were calculated using the two models described in Seq. 4.2 & 4.3. Total annual costs of 8,214,855 and 4,711,400 $/year were found for the acid and enzymatic hydrolysis routes respectively. This results in a price of 0.147 and 0.084 $/kg glucose for the acid and enzymatic hydrolysis route respectively assuming a plant lifetime of 20 years for both. The high capital expenditures for enzymatic hydrolysis come from the expensive distillation equipment, whereas the higher operational expenditures are caused by the high temperature that is required for the reaction to occur. In this process, 38% of the OPEX accounts for cellulase costs, as 44% of the OPEX accounts for raw materials, of which 87% account for cellulase costs. The analysis was carried out using a 13% enzyme concentration (w/w), derived from experimental results. However, it is possible that a lower enzyme concentration, perhaps with a longer production time, could be equally effective, potentially reducing operational costs significantly. Given that enzyme costs account for 38% of the OPEX of the glucose production process, optimising enzyme usage could increase economic viability. Moreover, adjustments in the buffer ratio and enzyme concentration could also further reduce production costs, considering their substantial impact on the process economics.

Table 6: Calculation of CAPEX, OPEX, and costs per kg of glucose via the acid and enzymatic hydrolysis route

Production of glucose from TC by acid hydrolysis of cellulose		
CAPEX	5,303,000	$
OPEX	7,949,705	$/year
Total yearly costs	8,214,855	$/year
Costs per kg	0.147	$/kg
Production of glucose from TC by enzymatic hydrolysis of cellulose		
CAPEX	8,728,000	$
OPEX	4,275,000	$/year
Total yearly costs	4,711,400	$/year
Costs per kg	0.084	$/kg

For the fermentation model producing phenylalanine from glucose, the glucose price for enzymatic hydrolysis was used (0.084 $/kg). Capital and operating expenditures were found to be 114,671,000 and 72,037,000 $ respectively. As the payback time is highly dependent on the value of phenylalanine, an analysis was carried out by running the model with several prices for phenylalanine (Fig. 24). It was found that the process has a payback time of 40 years with a phenylalanine price of 7.5 euros and that as the price increases, the payback time significantly decreases. Using the analysis, the process was found economically feasible for a payback time between 15-25 years, meaning that the price of phenylalanine lies between 7.5-8.0 $/kg, currently (with a dollar/euro rate of 1/0.92) corresponding to ∼6.87-7.33 euros/kg. The value of phenylalanine for use in alkyds should be within this range or higher for the process to be economically viable. The decision to opt for enzymatic over acid hydrolysis is influenced by various factors, and any changes in these factors could change the preference. Although enzymatic hydrolysis offers a higher yield (a 4.5-fold increase), it requires substantially longer reaction times (24 times longer) compared to acid hydrolysis. However, the lower operating temperature for enzymatic hydrolysis results in reduced energy costs and potentially lower reactor costs, despite the necessity for larger or more reactors due to the lower efficiency of the process. The assumption that enzymatic hydrolysis reactors are half as expensive per cubic metre significantly influences operational expenditures, and makes competition for glucose by acid hydrolysis harder. These assumptions should be taken into account when interpreting the results.

When returning to the other production scales of interest: 1 and 5 kton/year; as these are lower than the production scale for which the model was built for (8,000 kton/year), it is assumed that the price of phenylalanine is higher for these scenarios. Therefore, the decision was made not to change the whole model, but to assume the price of phenylalanine using the power law and a plant lifetime of 20 years, on a scale of 8,000 MT/year, the value of phenylalanine has to be 7.75 $/kg for the process to reach this payback time and be economically viable. To calculate capital costs for a different scale, the power law was used for capital expenditures with an exponent of 0.6, typical for equipment used for biochemistry purposes. Operational expenditures were defined by assuming a linear relation between capacity and OPEX. Phenylalanine prices of 10.65 and 9.87 $/kg were found for production scales of 1 and 5 kton/year respectively. Corresponding with ∼9.78 and 9.06 €/kg respectively with the current exchange values.

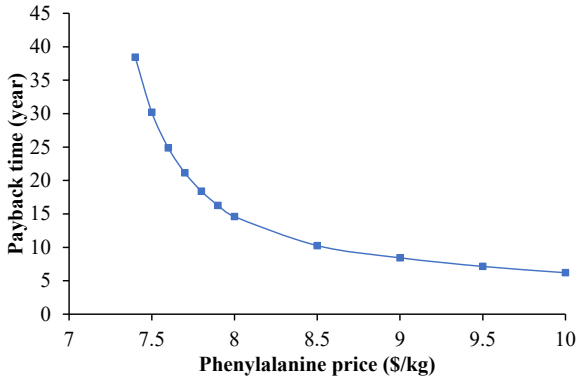

Figure 24: Graph of the payback time of the phenylalanine fermentation for phenylalanine prices ranging between 7.4-10$/kg

Table 7: CAPEX, OPEX, total annual costs and phenylalanine price calculated for phenylalanine production on a scale of 1 and 5 kton/year

1 kton/year		
CAPEX	32,930,597	$
OPEX	9,004,625	$/year
Total annual costs	10,651,155	$/year
Phenylalanine price	10.65	$/kg
5 kton/year		
CAPEX	86,493,129	$
OPEX	45,023,125	$/year
Total annual costs	49,347,781	$/year
Phenylalanine price	9.87	$/kg

5 Discussion

5.1 Theoretical implications

Production of glucose from cellulose

The observed optimal enzyme concentration of 13% facilitated a glucose yield nearly as high as that achieved with an excessive amount of enzyme (30%), suggesting efficient use of cellulase for hydrolysis. Although the yield achieved was approximately 70% in all cellulose sources, it was lower than the 90% yield commonly associated with enzymatic hydrolysis of pure cellulose (Yeh et al., 2010). The composition analysis revealing that tertiary cellulose consists of 60% cellulose indicates the potential for substantial glucose production.

The comparison between glucose production from washed and unwashed tertiary cellulose showed no significant difference, suggesting that the presence of noncellulosic materials in tertiary cellulose does not significantly impact the enzymatic hydrolysis efficiency. This aligns with the understanding that enzymatic hydrolysis, due to its specificity and mild operating conditions, can effectively break down cellulose into glucose with minimal susceptibility and formation of inhibitors or by-products (Walker and Wilson, 1991). However, the normalisation approach chosen in this study could have obscured potential variations in glucose yield between cellulose and tertiary cellulose sources, which requires further investigation.

Enzymatic hydrolysis in the presence of a phosphate buffer produced higher glucose levels compared to an acetate buffer, contrary to existing studies that favour the acetate buffer due to its compatibility with the optimal pH range of cellulase (Cheng, 1998). This unexpected result suggests that other factors might play a role in the influence of enzyme activity.

Production of phenylalanine from glucose

The successful application of UV mutagenesis and selection using an amino acid analogue (F-phenylalanine) led to the development of a *C. glutamicum* mutant with enhanced capabilities for the production of phenylalanine. This mutant achieved a maximum production rate of 0.46 g/L phenylalanine, corresponding to 0.046 g phenylalanine/g glucose. This production rate is relatively low, compared to metabolic engineering efforts that have historically achieved phenylalanine production of up to 20 g/L through various strain optimisation techniques (Shu and Liao, 2002). Thus, random mutagenesis and strain isolation with F-phenylalanine was found to be effective in terms of phenylalanine production, but it has a low chance of obtaining a strain producing a high yield. The phenylalanine production levels observed when the mutant was grown on G-PC-AC, G-TC-AC, and G-WTC-AC substrates were not significantly different, suggesting that the different substrates did not significantly affect the mutant's phenylalanine production capabilities, underscoring the mutant strain's robustness and its utilisation of available glucose. No significant variance in production, growth, or glucose consumption was observed when the strain was grown on G-TC-PH, G-TC-AC, G-PC-PH, G-PC-AC, and G-TC-AH. Where phenylalanine yields on the G-TC-AH and G-PC-AC substrates exceeded those of pure glucose (approximately 0.55 g/L), highlighting the potential of these substrates for the production of phenylalanine. This could indicate improved metabolic efficiency or altered regulatory responses in the mutant strain, allowing for enhanced phenylalanine biosynthesis. In all experiments, glucose was found to be the growth-limiting component, in line with the literature, and showing potential for fed-batch fermentation (Van Balken, 1997), (Pérez-Sánchez et al., 2021).

Before the experiments for analysis of the metabolite and growth parameters on different sub-

strates, the production was observed with pure glucose as a substrate. Interestingly, in trials with different substrates, pure glucose did not show growth. The identical media composition across all variants, except for the glucose source, could potentially be an issue with one of the trace elements. It could be speculated that a necessary trace element, possibly present in the tertiary cellulose, was absent or inactivated in the media. As the same syringe was used for filtering the glucose from all cellulose sources, it could be that the trace element present in tertiary cellulose was transferred to the glucose from pure cellulose, explaining growth on all substrates except pure glucose.

Economic feasibility

The economic analysis revealed that glucose production from tertiary cellulose is significantly more cost effective when using enzymatic hydrolysis compared to acid hydrolysis when producing the same amount of glucose, with production costs amounting to 0.084 $/kg and 0.147 $/kg for enzymatic and acid hydrolysis respectively, in contrast to the literature, where high enzyme costs make competition with acid hydrolysis difficult (Rinaldi and Schüth, 2009),(Aden and Foust, 2009). Lower costs in this model are operationalised by enzyme production by fermentation while using the relatively cheap produced glucose as a carbon source. Furthermore, the result showed that the production of phenylalanine, using glucose obtained from tertiary cellulose through enzymatic hydrolysis at production scales of 8, 5, and 1 kton/year are economically attractive starting from a phenylalanine value of 7.12, 9.06, and 9.78 €/kg respectively and when considering a 20-year payback period.

5.2 Managerial implications

The model applied in this research indicates that the process is too costly for practical large-scale application. To enhance economic feasibility, the mass balance parameters could be reassessed to confirm, as they were now based on the literature. Furthermore, exploring alternative substrates with higher cellulose content and greater availability could be interesting, as the extensive use of wastewater in the current process significantly increases the transportation costs of the different WWTPs, undermining economic viability. Transitioning to readily available waste paper streams as a cellulose source could present a cost-effective and sustainable alternative, potentially reducing transportation expenses and improving the overall sustainability and cost efficiency of the process.

5.3 Further research

Further research could streamline and optimise the bioprocesses involved in phenylalanine production. Investigating the potential for sterilising only cellulose to prevent microbial growth could offer an energy-efficient alternative to the current use of phosphate buffer. Exploring the effect of acid hydrolysis as a pretreatment in this context, despite the dispersed nature of the cellulose, could uncover opportunities to enhance yield. Additionally, verifying the necessity of adding ammonium, considering the possible presence of urea-derived ammonium in the material, could simplify the process and reduce environmental impact.

A more detailed analysis is needed using HPLC to understand the impact of different glucose sources and potential impurities on the metabolic pathway. Further exploration into the use of auxotrophic mutants could lead to significant improvements in production efficiency. Lastly, assessing the benefits of removing impurities upstream to facilitate downstream purification and reduce energy consumption could provide a more efficient overall process.

6 Conclusion

This study investigated the enzymatic hydrolysis of tertiary cellulose to produce glucose and its subsequent fermentation to phenylalanine using a *C. glutamicum* strain. The results indicate that a concentration of 13% cellulase is nearly as effective as the excess concentration, achieving a yield of approximately 70% glucose from pure cellulose sources, being lower than the 90% yield reported in prior studies. The glucose yields were consistent between washed and unwashed tertiary cellulose, with no significant differences in terms of glucose production when the use of a phosphate and acetate buffer was compared.

The phenylalanine-producing *C. glutamicum* mutant, developed through UV mutagenesis, demonstrated the production of phenylalanine without significant differences between various glucose substrates derived from cellulose. The experimental results revealed that the glucose source did not significantly impact phenylalanine production, suggesting that the engineered strain efficiently converts glucose to phenylalanine regardless of the glucose's cellulose origin.

Economically, the analysis supports the feasibility of producing phenylalanine from tertiary cellulose-derived glucose via enzymatic hydrolysis. The cost-effectiveness of enzymatic hydrolysis over acid hydrolysis was found to be evident, with the operational and environmental benefits also favouring the former. Production costs were found to be economically viable on a production scale of 1, 5, and 8 kton/year for a phenylalanine value of 10.65, 9.87, and 7.5 $/kg respectively, showing the potential for scalable phenylalanine production from wastewater-derived tertiary cellulose. However, while the process shows promise for industrial-scale production, the cost implications for downstream applications, such as alkyd resin synthesis, remain a concern. The target cost for making the production of alkyds from phenylalanine economically attractive would be in the range of a few euros per kilogramme. Given current cost projections, it is uncertain whether the production of phenylalanine from tertiary cellulose can meet these price points at the analysed scales, suggesting the need for further optimisation or alternative strategies to reduce costs and enhance economic attractiveness.

References

Spyridon Achinas, Nienke Leenders, Janneke Krooneman, and Gerrit Jan Willem Euverink. Feasibility assessment of a bioethanol plant in the northern netherlands. *Applied Sciences*, 9(21):4586, 2019.

Andy Aden and Thomas Foust. Technoeconomic analysis of the dilute sulfuric acid and enzymatic hydrolysis process for the conversion of corn stover to ethanol. *Cellulose*, 16: 535–545, 2009.

Ahmed Shawki Ahmed, Gholamreza Bahreini, Dang Ho, Ganesh Sridhar, Medhavi Gupta, Coos Wessels, Pim Marcelis, Elsayed Elbeshbishy, Diego Rosso, Domenico Santoro, et al. Fate of cellulose in primary and secondary treatment at municipal water resource recovery facilities. *Water Environment Research*, 91(11):1479–1489, 2019.

V Anoop Kumar, R Suresh Chandra Kurup, C Snishamol, and G Nagendra Prabhu. Role of cellulases in food, feed, and beverage industries. *Green Bio-processes: Enzymes in Industrial Food Processing*, pages 323–343, 2018.

Carsten Bäumchen, Arnd Knoll, Bernward Husemann, Juri Seletzky, Bernd Maier, Carsten Dietrich, Ghassem Amoabediny, and Jochen Büchs. Effect of elevated dissolved carbon dioxide concentrations on growth of corynebacterium glutamicum on d-glucose and l-lactate. *Journal of biotechnology*, 128(4):868–874, 2007.

Simone Brethauer and Charles E Wyman. Continuous hydrolysis and fermentation for cellulosic ethanol production. *Bioresource technology*, 101(13):4862–4874, 2010.

Currell R.C. Brian, Van Dam, Mieras, and Biotol Partners Staff. *Biotechnological Innovations in Chemical Synthesis - 8.6.1 Process Economics of the Fermentative Production of L-Phenylalanine.* Elsevier, 1997. Retrieved from https://app.knovel.com/hotlink/pdf/id:kt005BQ525/biotechnological-innovations/process-economics-fermentative.

Cheanyeh Cheng. Cellulase activity in different buffering media during waste paper hydrolysis by hplc. *Journal of the Chinese Chemical Society*, 45(5):679–688, 1998.

L De Boer and L Dijkhuizen. Microbial and enzymatic processes for l-phenylalanine production. In *Microbial Bioproducts*, pages 1–27. Springer, 2005.

Dongqin Ding, Yongfei Liu, Yiran Xu, Ping Zheng, Haixing Li, Dawei Zhang, and Jibin Sun. Improving the production of l-phenylalanine by identifying key enzymes through multi-enzyme reaction system in vitro. *Scientific reports*, 6(1):32208, 2016.

Gerrit Jan Willem Euverink. Biosynthesis of phenylalanine and tyrosine in the methylotrophic actinomycete amycolatopsis methanolica. 1995.

AM Fazel and RA Jensen. Aromatic aminotransferases in coryneform bacteria. *Journal of Bacteriology*, 140(2):580–587, 1979.

Gerardo Gomez, Michael J Pikal, and Naír Rodríguez-Hornedo. Effect of initial buffer composition on ph changes during far-from-equilibrium freezing of sodium phosphate buffer solutions. *Pharmaceutical research*, 18:90–97, 2001.

Hiroshi Hagino and Kiyoshi Nakayama. L-phenylalanine production by analog-resistant mutants of corynebacterium glutamicum. *Agricultural and Biological Chemistry*, 38(1):157–161, 1974.

Mélanie Hall, Prabuddha Bansal, Jay H Lee, Matthew J Realff, and Andreas S Bommarius. Cellulose crystallinity–a key predictor of the enzymatic hydrolysis rate. *The FEBS journal*, 277(6):1571–1582, 2010.

Edwin Haslam. Shikimic acid: metabolism and metabolites. *(No Title)*, 1993.

Klaus M Herrmann. The shikimate pathway: early steps in the biosynthesis of aromatic compounds. *The Plant Cell*, 7(7):907, 1995.

Ad Hofland. Alkyd resins: From down and out to alive and kicking. *Progress in Organic Coatings*, 73(4):274–282, 2012.

Ikhazuagbe H Ifijen, Muniratu Maliki, Ifeanyi J Odiachi, Oscar N Aghedo, and Ewanole B Ohiocheoya. Review on solvents based alkyd resins and water borne alkyd resins: impacts of modification on their coating properties. *Chemistry Africa*, 5(2):211–225, 2022.

Masato Ikeda, Akio Ozaki, and Ryoichi Katsumata. Phenylalanine production by metabolically engineered corynebacterium glutamicum with the phea gene of escherichia coli. *Applied microbiology and biotechnology*, 39:318–323, 1993.

Intelligen, Inc. Superpro designer examples. `https://www.intelligen.com/products/superpro-examples/`. Accessed: 2024-03-01.

Toshio Iwasaki, Yoshiharu Miyajima-Nakano, Risako Fukazawa, Myat T Lin, Shin-ichi Matsushita, Emi Hagiuda, Alexander T Taguchi, Sergei A Dikanov, Yumiko Oishi, and Robert B Gennis. Escherichia coli amino acid auxotrophic expression host strains for investigating protein structure–function relationships. *The journal of biochemistry*, 169(4):387–394, 2021.

Mohammed Nazeer Khan, Mark Lacroix, Coos Wessels, and Miet Van Dael. Converting wastewater cellulose to valuable products: A techno-economic assessment. *Journal of Cleaner Production*, 365:132812, 2022.

Adrianus Jozephus Hendricus Lansbergen, Cornelis Eme Koning, Paulus Franciscus Anna Buijsen, Johannes Wilhelmus Maria Hendriks, and Alwin Papegaaij. Polymer and composition, apr 2015. URL `https://patents.google.com/patent/WO2015052342A1/en`.

Mathieu Lapointe, Heidi Jahandideh, Jeffrey M Farner, and Nathalie Tufenkji. Super-bridging fibrous materials for water treatment. *npj Clean Water*, 5(1):11, 2022.

Nelson Libardi, Luciana Porto de Souza Vandenberghe, Zulma Sarmiento Vásquez, Valcineide Tanobe, Júlio César de Carvalho, and Carlos Ricardo Soccol. A non-waste strategy for enzymatic hydrolysis of cellulose recovered from domestic wastewater. *Environmental Technology*, 43(10):1503–1512, 2022.

Pedro A Lira-Parada, Andrea Tuveri, Gerd M Seibold, and Nadav Bar. Comparison of noninvasive, in-situ and external monitoring of microbial growth in fed-batch cultivations in corynebacterium glutamicum. *Biochemical Engineering Journal*, 170:107989, 2021.

Ranbin Liu, Yaxuan Li, Mengbo Zhang, Xiaodi Hao, and Jie Liu. Review on the fate and

recovery of cellulose in wastewater treatment. *Resources, Conservation and Recycling*, 184: 106354, 2022.

HP Loh, Jennifer Lyons, and Charles W White. Process equipment cost estimation, final report. Technical report, National Energy Technology Lab.(NETL), Morgantown, WV (United States), 2002.

Tina Lütke-Eversloh and Gregory Stephanopoulos. Feedback inhibition of chorismate mutase/prephenate dehydrogenase (tyra) of escherichia coli: generation and characterization of tyrosine-insensitive mutants. *Applied and Environmental Microbiology*, 71(11):7224–7228, 2005.

Mary Mandels, Lloyd Hontz, and John Nystrom. Enzymatic hydrolysis of waste cellulose. *Biotechnology and bioengineering*, 16(11):1471–1493, 1974.

Silvia Morales-delaRosa, Jose M Campos-Martin, and Jose LG Fierro. Optimization of the process of chemical hydrolysis of cellulose to glucose. *Cellulose*, 21:2397–2407, 2014.

Hao Niu, Ruirui Li, Quanfeng Liang, Qingsheng Qi, Qiang Li, and Pengfei Gu. Metabolic engineering for improving l-tryptophan production in escherichia coli. *Journal of Industrial Microbiology and Biotechnology*, 46(1):55–65, 2019.

Novozymes. Cellic ctec and htec2—enzymes for hydrolysis of lignocellulosic materials. *Novozymes A/S, Luna*, 1668(01), 2010.

Janna Pachuski, Bernard Fried, and Joseph Sherma. Hptlc analysis of amino acids in biomphalaria glabrata infected with schistosoma mansoni. *Journal of liquid chromatography & related technologies*, 25(13-15):2345–2349, 2002.

Minkyu Park and Shane A Snyder. Attenuation of contaminants of emerging concerns by nanofiltration membrane: rejection mechanism and application in water reuse. In *Contaminants of Emerging Concern in Water and Wastewater*, pages 177–206. Elsevier, 2020.

Amaury Pérez-Sánchez, Elizabeth Ranero-González, Eddy J Pérez-Sánchez, and RUTDALI SEGURA-SILVA. Simulación del proceso de producción de l-fenilalanina por la ruta fermentativa utilizando el simulador superpro designer®. *Revista EIA*, 18(35):220–234, 2021.

Yungeng Qi, Yanzhu Guo, Afroza Akter Liza, Guihua Yang, Mika H Sipponen, Jiaqi Guo, and Haiming Li. Nanocellulose: a review on preparation routes and applications in functional materials. *Cellulose*, 30(7):4115–4147, 2023.

Roberto Rinaldi and Ferdi Schüth. Acid hydrolysis of cellulose as the entry point into biorefinery schemes. *ChemSusChem: Chemistry & Sustainability Energy & Materials*, 2(12): 1096–1107, 2009.

Fabien Robert-Peillard, Elodie Mattio, Aïnhoa Komino, Jean-Luc Boudenne, and Bruno Coulomb. Development of a simple, low-cost and rapid thin-layer chromatography method for the determination of individual volatile fatty acids. *Analytical Methods*, 11(14):1891–1897, 2019.

Dutch Water Sector. Launch cellcap technology for cellulose recovery from wastewater. `https://www.dutchwatersector.com/news/`

launch-cellcap-technology-for-cellulose-recovery-from-wastewater, 2024. Accessed: 2024-02-08.

Chin-Hang Shu and Chii-Cherng Liao. Optimization of l-phenylalanine production of corynebacterium glutamicum under product feedback inhibition by elevated oxygen transfer rate. *Biotechnology and bioengineering*, 77(2):131–141, 2002.

Towering Skills. Cost indices, 2024. URL https://toweringskills.com/financial-analysis/cost-indices/. [Accessed on March 2, 2024].

LA Spano, J Medeiros, and MJUA Mandels. Enzymatic hydrolysis of cellulosic wastes to glucose. *Resource Recovery and Conservation*, 1(3):279–294, 1976.

Statista. Netherlands: monthly wholesale electricity price 2023, 2024. URL https://www.statista.com/statistics/1314549/netherlands-monthly-wholesale-electricity-price/. [Accessed on March 2, 2024].

Zhao-Yong Sun, Yue-Qin Tang, Shigeru Morimura, and Kenji Kida. Reduction in environmental impact of sulfuric acid hydrolysis of bamboo for production of fuel ethanol. *Bioresource technology*, 128:87–93, 2013.

KH Sreedhara Swamy and Julian J Jaffe. Isolation, partial purification and some properties of two acid proteases from adult dirofilaria immitis. *Molecular and biochemical parasitology*, 9(1):1–14, 1983.

Abiola Ezekiel Taiwo, Andykan Tom-James, and Paul Musonge. Economic assessment of cellulase production in batch and semi-batch solid-state fermentation processes. *International Journal of Low-Carbon Technologies*, 18:204–211, 2023.

JAM Van Balken. *Biotechnological innovations in chemical synthesis*. Butterworth-Heinemann, 1997.

LP Walker and DB Wilson. Enzymatic hydrolysis of cellulose: an overview. *Bioresource technology*, 36(1):3–14, 1991.

Qingshi Wu, Xue Du, Aiping Chang, Xiaomei Jiang, Xiaoyun Yan, Xiaoyu Cao, Zahoor H Farooqi, and Weitai Wu. Bioinspired synthesis of poly (phenylboronic acid) microgels with high glucose selectivity at physiological ph. *Polymer Chemistry*, 7(42):6500–6512, 2016.

An-I Yeh, Yi-Ching Huang, and Shih Hsin Chen. Effect of particle size on the rate of enzymatic hydrolysis of cellulose. *Carbohydrate polymers*, 79(1):192–199, 2010.

Ryo Yokoyama, Marcos VV de Oliveira, Bailey Kleven, and Hiroshi A Maeda. The entry reaction of the plant shikimate pathway is subjected to highly complex metabolite-mediated regulation. *The Plant Cell*, 33(3):671–696, 2021.

A Appendix A: Photos

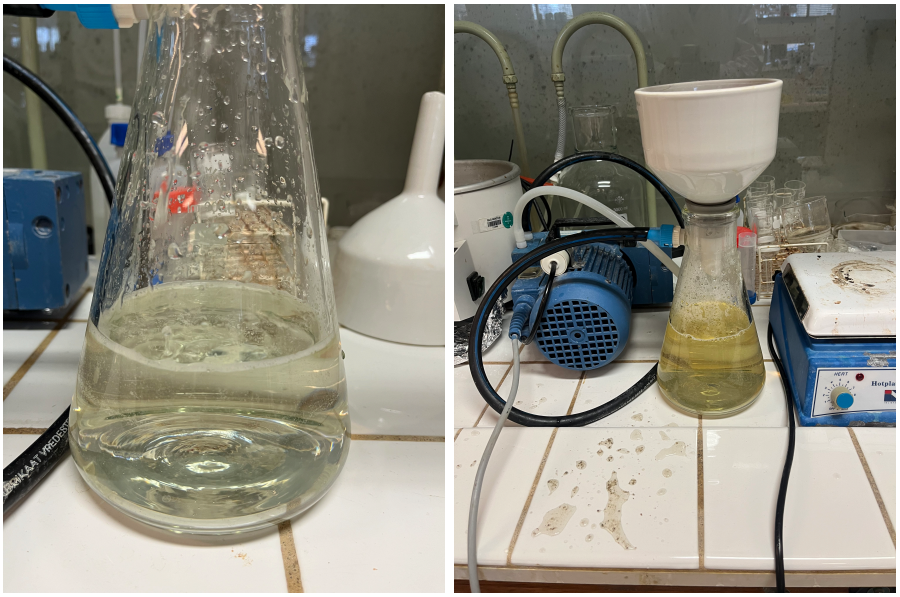

Figure 25: Resulting water in Büchner set-up after washing for one hour (left) and after one hour in the ultrasonic bath (right)

Figure 26: Picture of tertiary cellulose before (left) and after (right) washing

Figure 27: Set-up of tube rotator in incubator

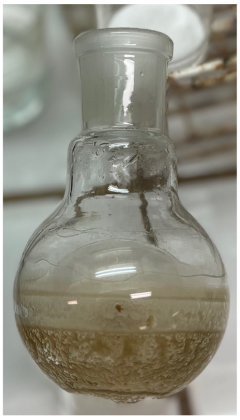

Figure 28: Crystallized glucose after vacuum distillation

Figure 29: TLC amino acids assay with a:washed tertiary cellulose, and b:tertiary cellulose

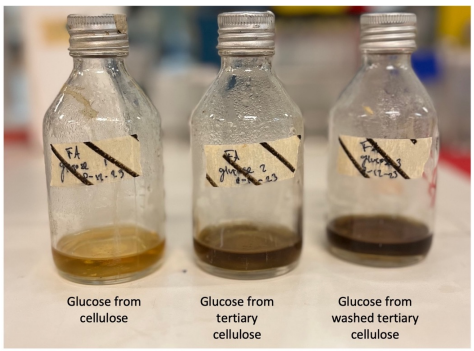

Figure 30: Glucose from pure, tertiary and washed tertiary cellulose after autoclaving at 121 degrees for 15 minutes

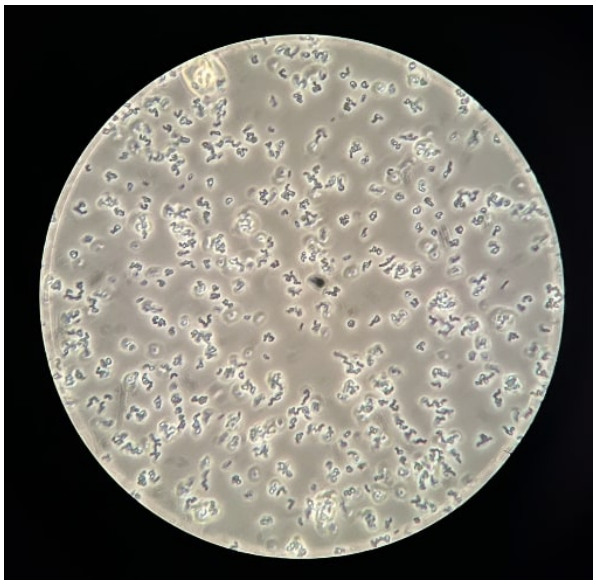

Figure 31: C. glutamicum in BHI under a microscope at x1000 magnitude

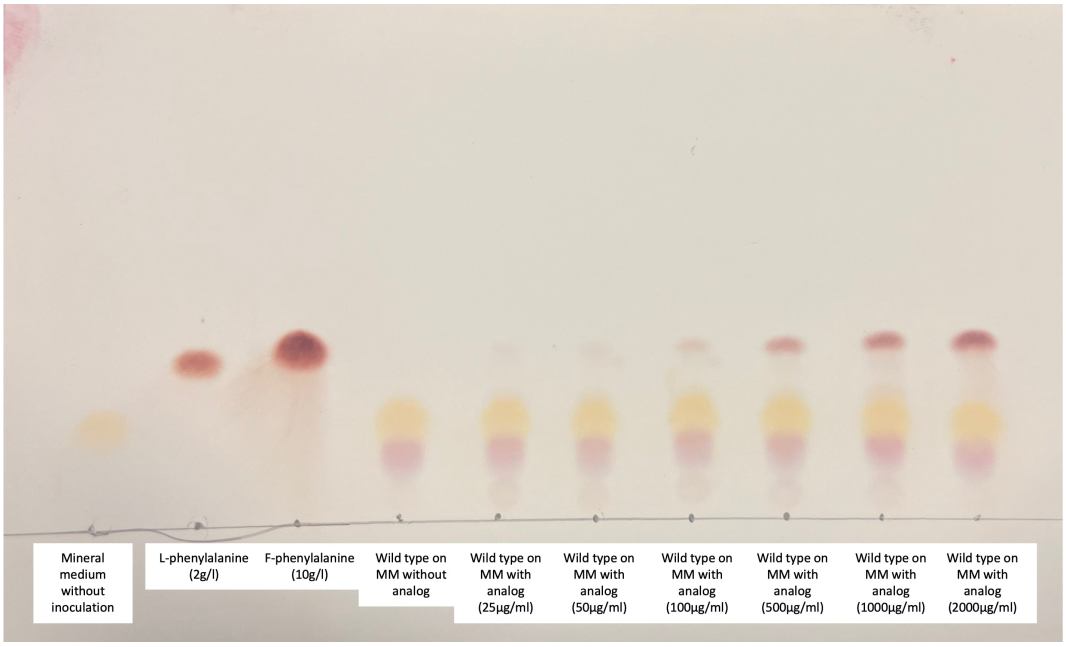

Figure 32: TLC amino acids assay with MM, L-phenylalanine (2 g/l), F-phenylalanine (10 g/l), and growth after 46 hours with 0, 25, 50, 100, 500, 1000, and 2000 µg/ml analog

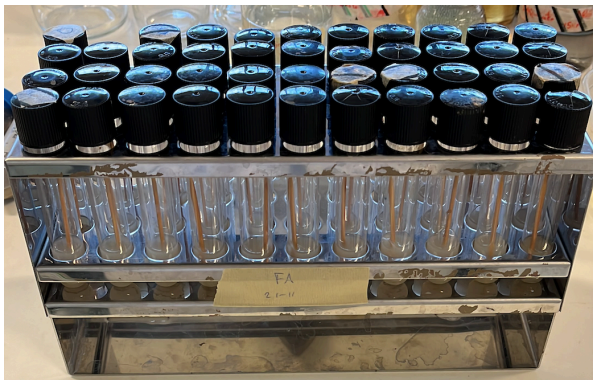

Figure 33: 10 ml tube rack consisting of 43 isolated strains after 3 days at 30°C in an incubator at 100 rpm

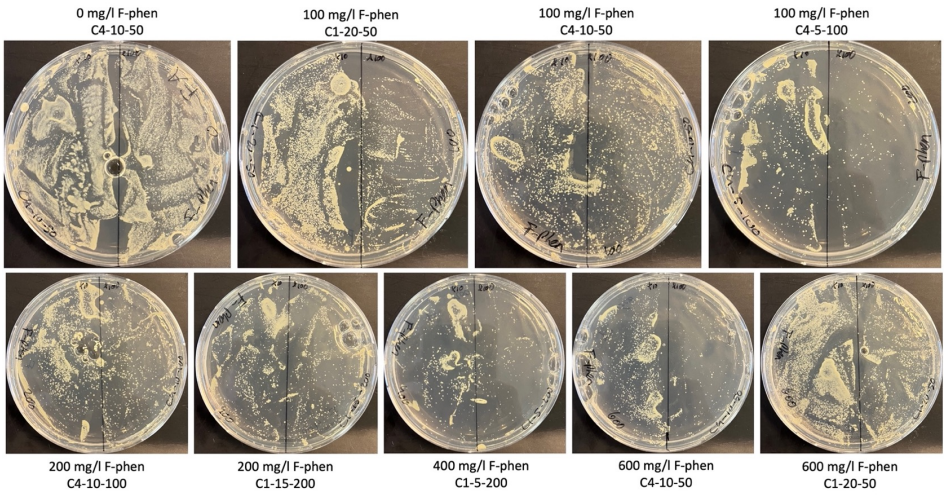

Figure 34: Agar plates with isolated colonies after second UV mutagenesis

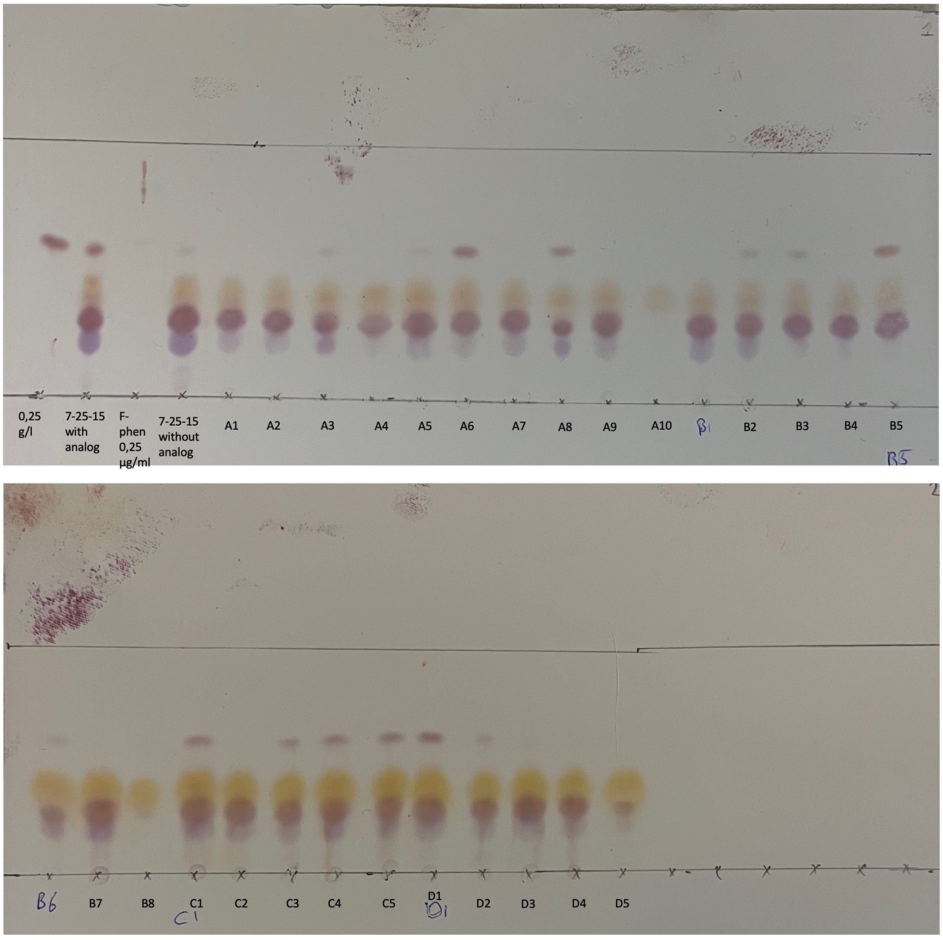

Figure 35: TLC amino acids assay of obtained strains after isolation of the first mutated phenylalanine-producing strain

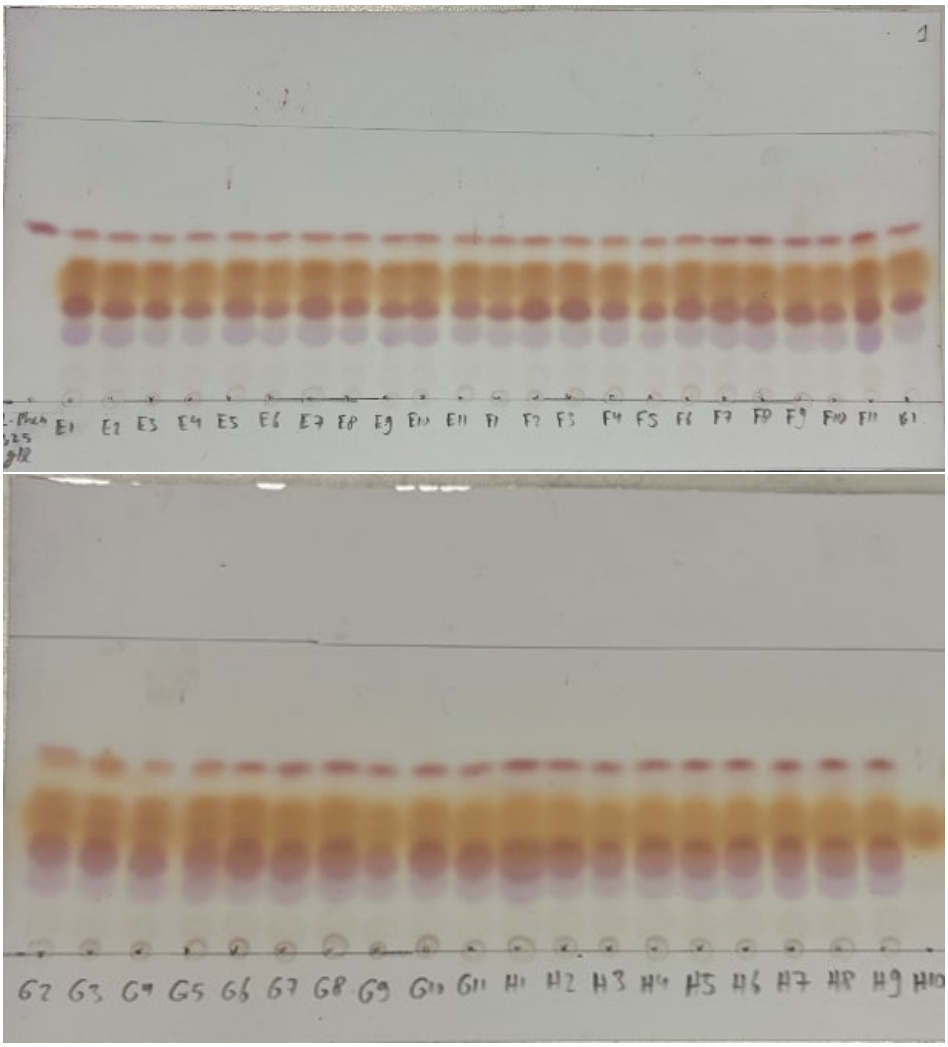

Figure 36: TLC amino acids assay of isolated strains in MM in the absence of F-phenylalanine after the second mutagenesis

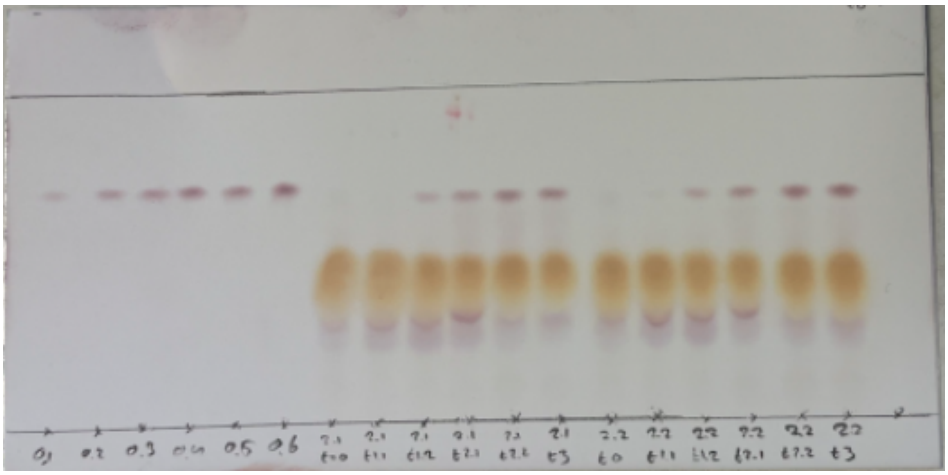

Figure 37: Result of amino acid TLC assay showing standard concentrations of phenylalanine (left) and the production profile of H1 on MM containing G-TC-AC over time

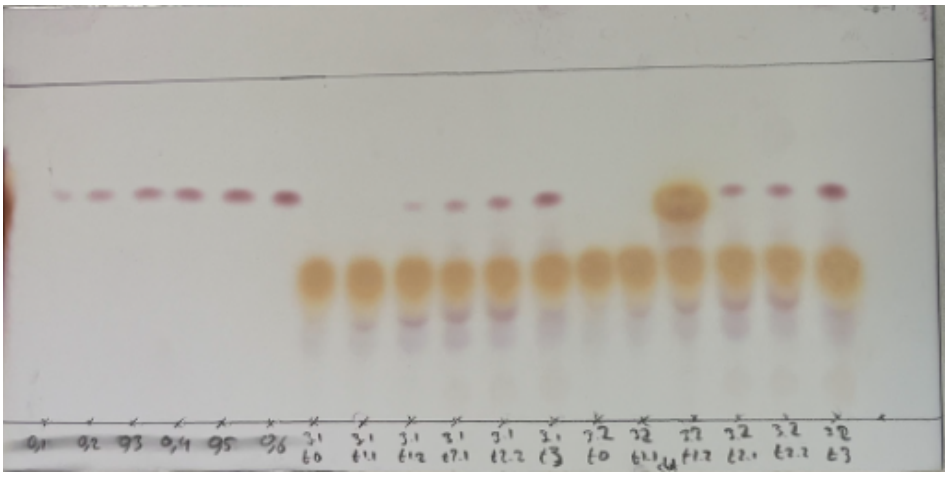

Figure 38: Result of amino acid TLC assay showing standard concentrations of phenylalanine (left) and the production profile of H1 on MM containing G-PC-AC over time

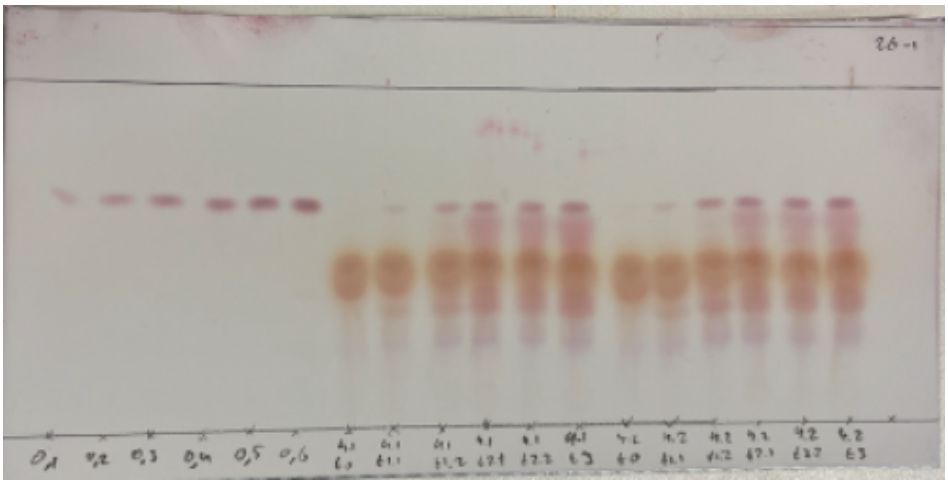

Figure 39: Result of amino acid TLC assay showing standard concentrations of phenylalanine (left) and the production profile of H1 on MM containing G-TC-PH over time

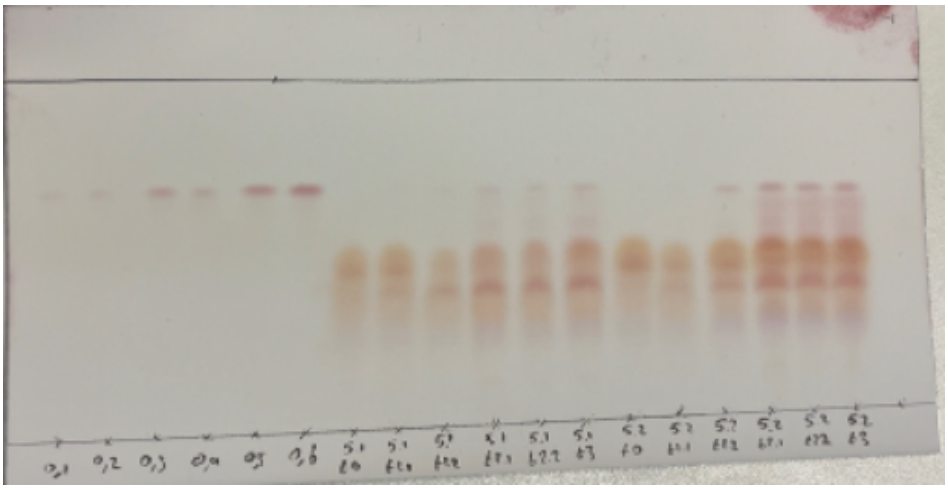

Figure 40: Result of amino acid TLC assay showing standard concentrations of phenylalanine (left) and the production profile of H1 on MM containing G-PC-PH over time

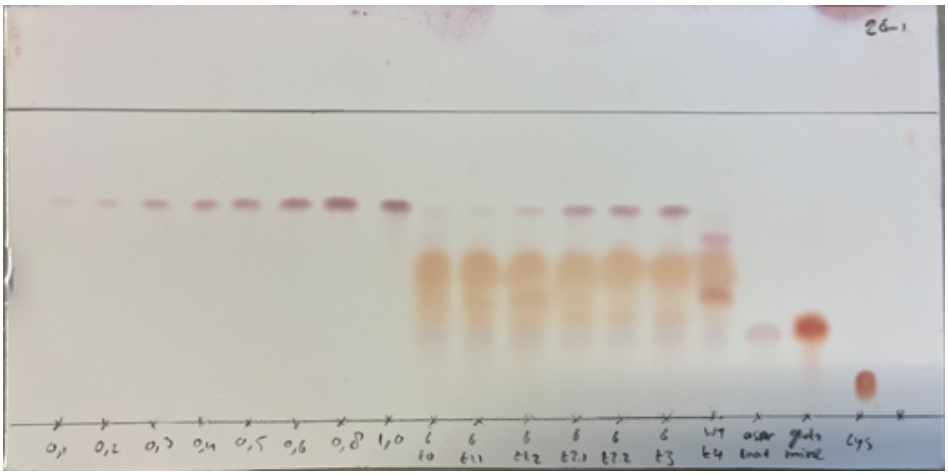

Figure 41: Result of amino acid TLC assay showing standard concentrations of phenylalanine (left) and the production profile of H1 on MM containing G-TC-AH over time

B Appendix B: Tables

Table 8: Glucose yield obtained from differing cellulose sources with differing amounts of enzyme

		Yield (w/w %)				
Cellulose type	Enzyme (w/w)	t=0 h	t=24 h	t-48 h	t=72 h	t=96 h
Cellulose -	1.5	0%	5%	10%	14%	16%
Cellulose -	3	0%	7%	15%	20%	25%
Cellulose -	13	0%	24%	50%	70%	67%
Cellulose -	30	0%	26%	50%	72%	70%
Tertiary Cellulose -	1.5	0%	4%	8%	9%	11%
Tertiary Cellulose -	3	0%	5%	12%	13%	15%
Tertiary Cellulose -	13	0%	19%	37%	43%	42%
Tertiary Cellulose -	30	0%	16%	37%	44%	43%
Washed Tertiary Cellulose -	1.5	0%	5%	9%	10%	11%
Washed Tertiary Cellulose -	3	0%	6%	11%	13%	14%
Washed Tertiary Cellulose -	13	0%	20%	36%	41%	38%
Washed Tertiary Cellulose -	30	0%	23%	39%	41%	41%

Table 9: UV mutagenesis on agar plates with x1000 dilution and differing concentrations of analog and UV exposure time.

Plate	Analogue (g/ml)	Dilution	UV mutagenesis (s)	Growth after
1	0	X1000, 100 μL	0	2 days
2	25	X1000, 100 μL	15	-
3	25	X1000, 100 μL	30	-
4	25	X1000, 100 μL	45	-
5	25	X1000, 100 μL	60	-
6	25	X1000, 100 μL	0	2 days
7	50	X1000, 100 μL	15	-
8	50	X1000, 100 μL	30	-
9	50	X1000, 100 μL	45	-
10	50	X1000, 100 μL	60	-
11	50	X1000, 100 μL	0	2 days

Table 10: UV mutagenesis on agar plates with x100 dilution and differing concentrations of analog and UV exposure time.

Plate	Analogue (g/ml)	Dilution	UV mutagenesis (s)	Growth after
1	0	X100, 100 μL	0	2 days
2	25	X100, 100 μL	15	-
3	25	X100, 100 μL	30	-
4	25	X100, 100 μL	45	-
5	25	X100, 100 μL	60	-
6	25	X100, 100 μL	0	2 days
7	50	X100, 100 μL	15	-
8	50	X100, 100 μL	30	-
9	50	X100, 100 μL	45	-
10	50	X100, 100 μL	60	-
11	50	X100, 100 μL	0	2 days

Table 11: UV mutagenesis in conical flasks with differing concentrations of analog and UV exposure time.

Erlenmeyer	Analogue (g/ml)	Dilution	UV mutagenesis (s)	Growth after
1	25	x0, 50 μl	0	1 day
2	25	x0, 50 μl	15	2 days
3	25	x0, 50 μl	30	-
4	25	x0, 50 μl	60	-
5	50	x0, 50 μl	0	1 day
6	50	x0, 50 μl	15	2 days
7	50	x0, 50 μl	30	-
8	50	x0, 50 μl	60	-

Table 12: Dot volumes of (F-)phenylalanine dots on TLC plate of isolated strains after first mutagenesis

	Dot volume
0.25 g/l L-phenylalanine	23.4
0.5 g/l L-phenylalanine	38.5
0.25 g/ml F-phenylalanine	2.3
7-25-15 without analog	3.8
7-25-15 with analog	26.5
D2	10.7
A3	5.8
A5	2.6
A6	8.5
A8	10.6
B2	3.9
B3	5.4
B5	9.8
B6	3.0
C1	10.8
C3	6.7
C4	12.8
C5	9.0
D1	8.3

Table 13: Dot volumes of (F-)phenylalanine dots on amino acids TLC assay with the optical density of the corresponding strains

Strain	Dot volume	OD600
C1	1.3	
C4	3.8	
C1-5-50	6.8	2.57
C1-10-50	7.0	2.46
C1-15-50	5.7	2.42
C1-20-50	10.0	2.51
C1-5-100	11.7	2.46
C1-10-100	14.1	2.48
C1-15-100	11.0	1.89
C1-20-100	11.5	2.36
C1-5-200	19.6	2.33
C1-10-200	13.5	2.39
C1-15-200	19.5	2.2
C1-20-200	18.6	2.45
C4-5-50	7.9	2.59
C4-10-50	12.6	2.63
C4-15-50	8.3	2.45
C4-20-50	9.0	2.5
C4-5-100	15.5	2.73
C4-10-100	15.3	2.48
C4-15-100	9.5	2.36
C4-20-100	23.4	2.5
C4-5-200	13.6	2.37
C4-10-200	13.9	2.45
C4-15-200	15.2	2.6
C4-20-200	17.1	2.53
F-phen 50 µg/ml	2.4	
F-phen 100 µg/ml	6.7	
F-phen 200 µg/ml	11.2	

Table 14: Dot volume of (F-)phenylalanine dots on amino acid TLC sheet after isolation of second mutagenesis, with its corresponding optical density

Strain	Dot volume	OD600
L-phen 0.25 g/l	33.2	
E1	22.17	2.34
E2	22.36	2.23
E3	13.37	2.21
E4	16.6	2.29
E5	23.2	2.33
E6	16.63	2.4
E7	24.6	1.73
E8	15.05	2.29
E9	16.89	2.14
E10	24.7	2.23
E11	19.38	2.13
F1	16.11	2.43
F2	15.38	2.41
F3	25.29	2.39
F4	21.37	2.28
F5	13.66	2.44
F6	12.29	2.69
F7	19.51	2.31
F8	27.97	2.25
F9	15.86	2.44
F10	19.8	2.37
F11	22.95	2.26
G1	17.73	2.49
G2	28.32	2.48
G3	26.23	2.48
G4	11.71	2.35
G5	19.34	2.4
G6	13.78	2.26
G7	19.38	2.38
G8	20.58	2.38
G9	13.97	1.84
G10	20.49	2.2
G11	15.89	2.27
H1	15.03	2.31
H2	19.71	2.01
H3	15.97	2.44
H4	16.74	2.49
H5	17.9	2.48
H6	17.61	2.33
H7	18.91	2.46
H8	14.83	2.51
H9	20.03	2.31
H10	1.38	2.33

C Appendix C: Process diagrams

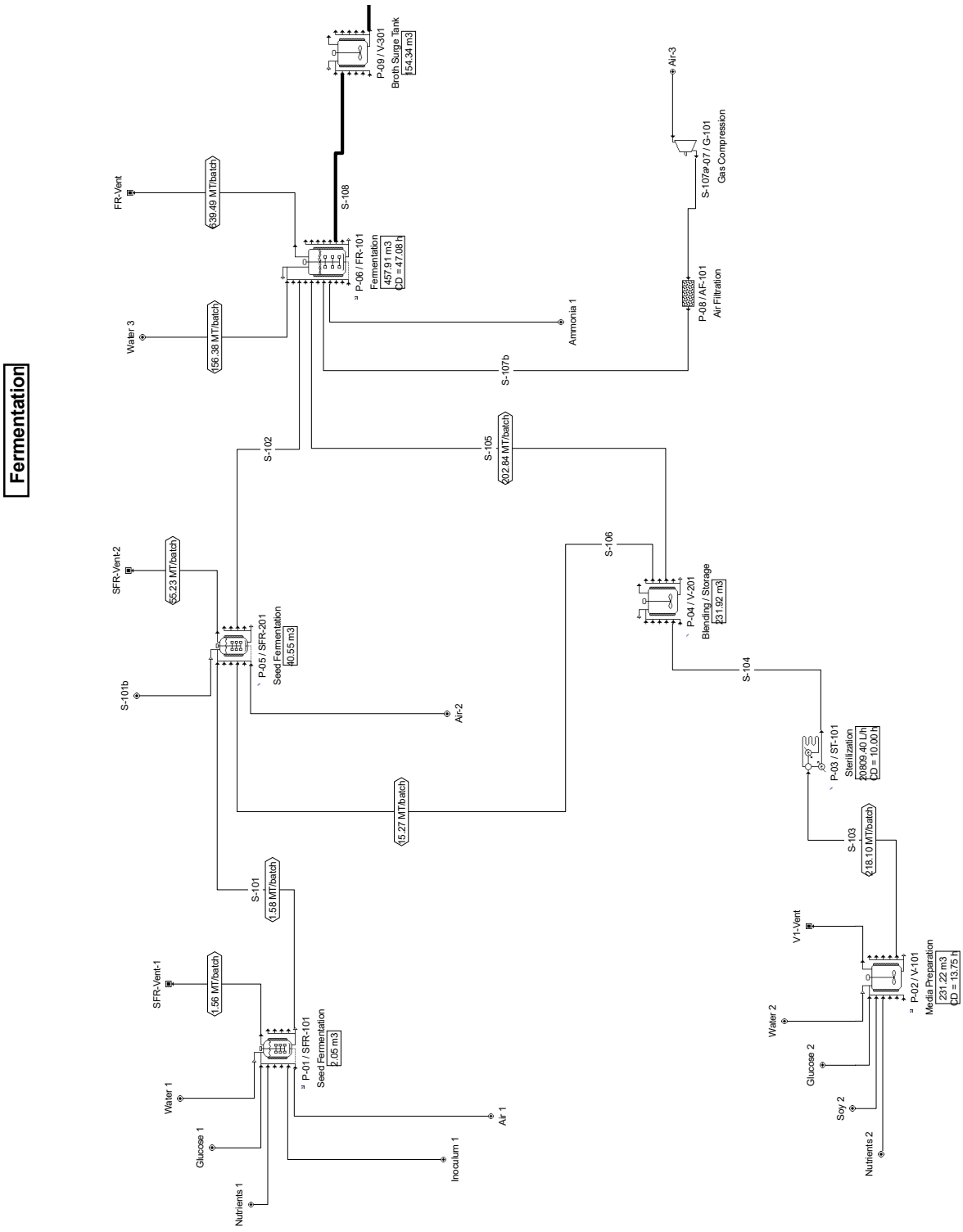

Figure 42: Fermentation part of the superpro process diagram for production of phenylalanine

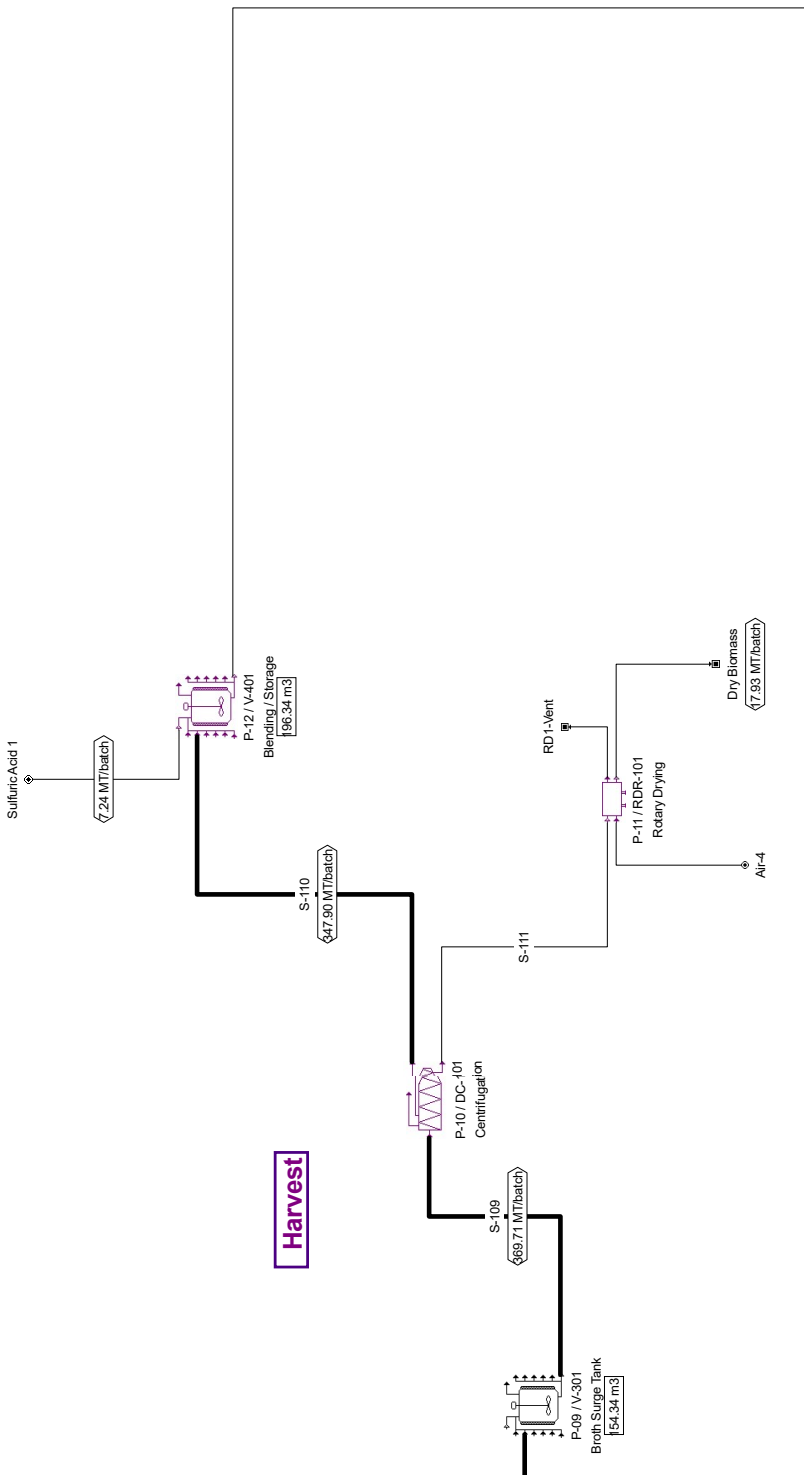

Figure 43: Harvest part of the superpro process diagram for production of phenylalanine

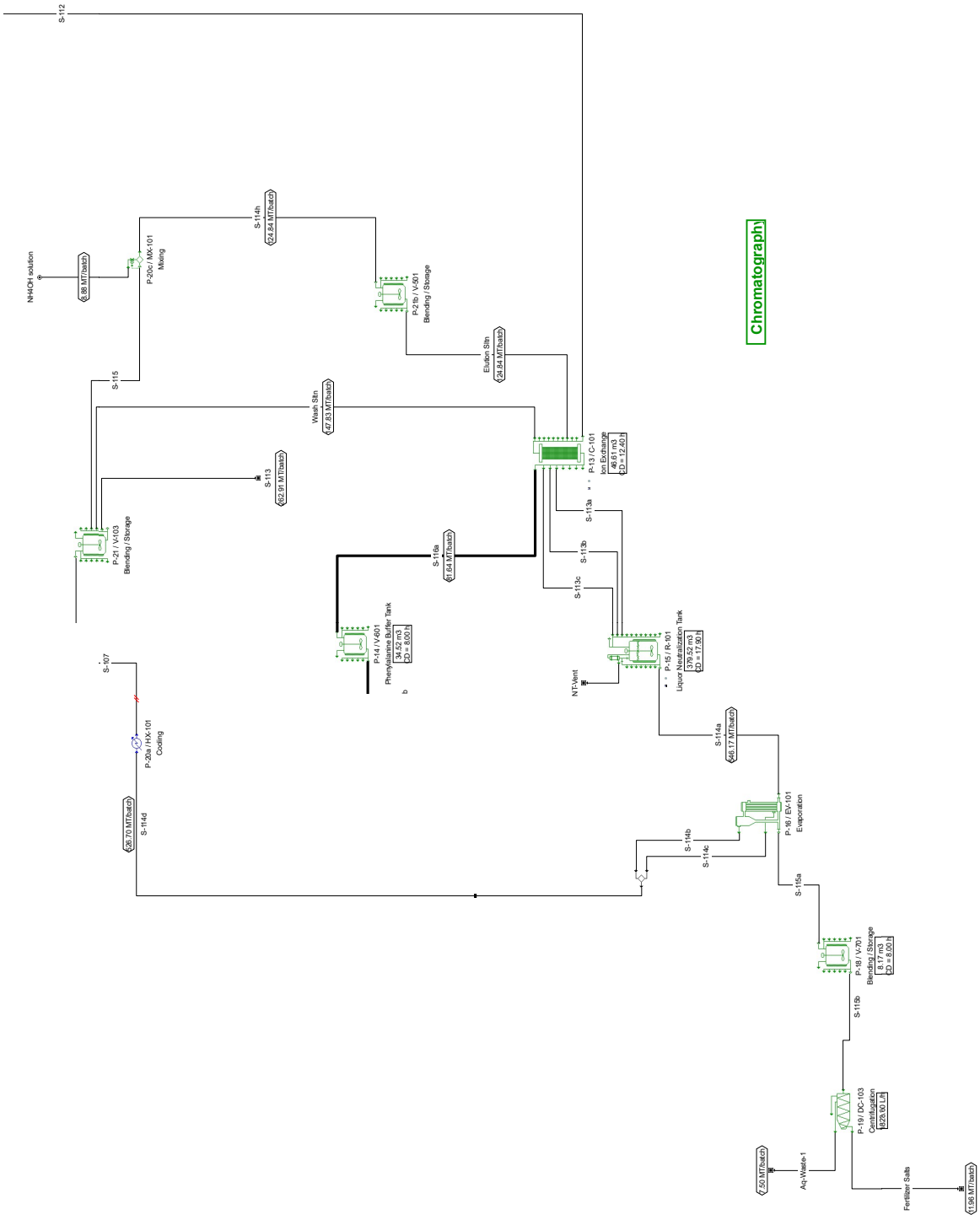

Figure 44: Chromatography part of the superpro process diagram for production of phenylalanine

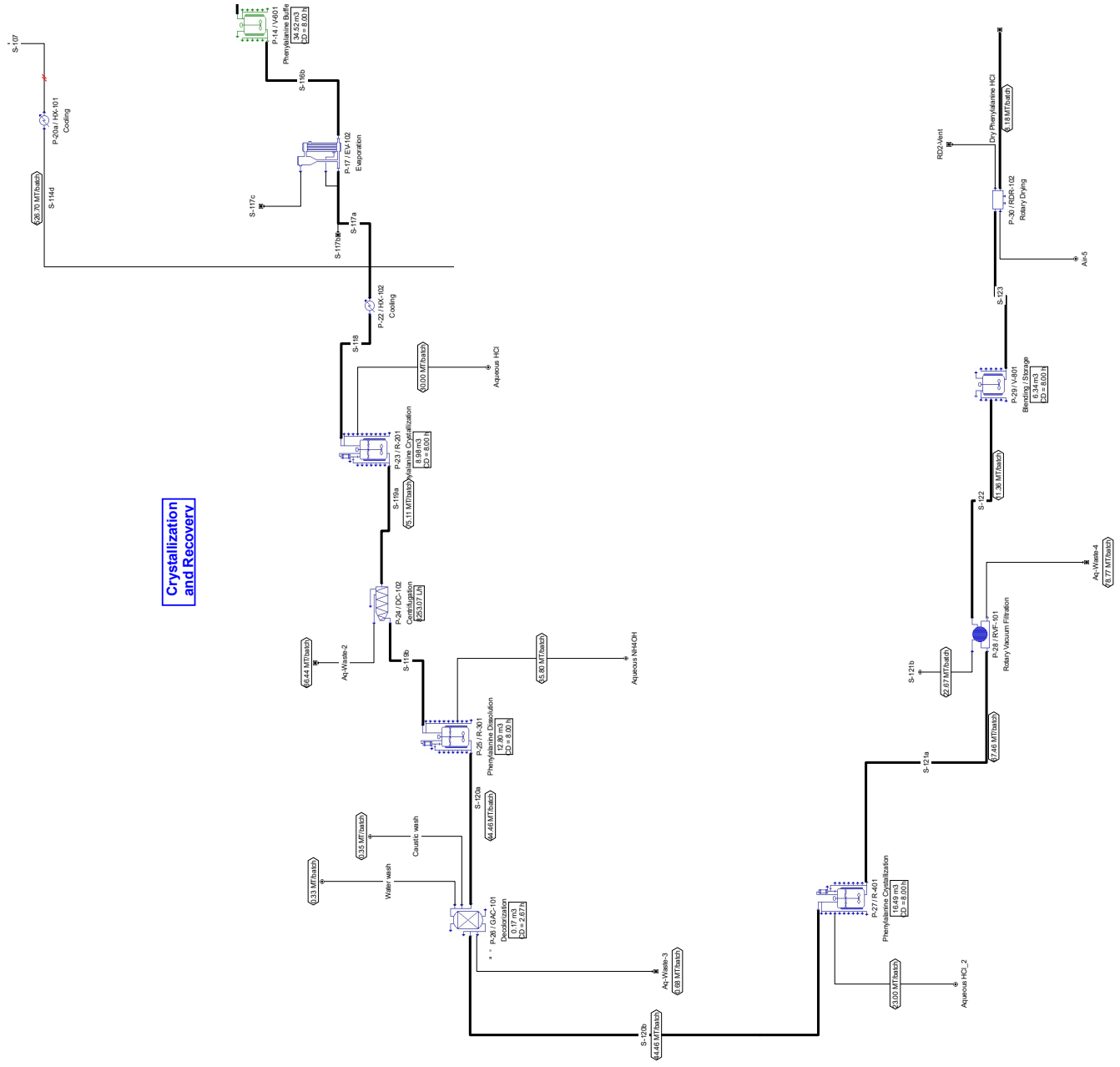

Figure 45: Crystallization part of the superpro process diagram for production of phenylalanine